Predicting Optimal Trim Configuration of Marine Vessels with respect to Fuel Usage

Stefán Pétursson

VERKFRÆÐI- OG NÁTTÚRUVÍSINDASVIÐ / SCHOOL OF ENGINEERING AND NATURAL SCIENCES

HÁSKÓLI ÍSLANDS / UNIVERSITY OF ICELAND

Predicting Optimal Trim Configuration of Marine Vessels with respect to Fuel Usage

Stefán Pétursson

A 60 ECTS credit units Master's thesis

Tutors

Professor Sven Þ. Sigurðsson

Professor Thomas Philip Rúnarsson

Faculty of Industrial Engineering, Mechanical Engineering and Computer Science

School of Engineering and Natural Sciences

University of Iceland

Reykjavik, June 2009

Predicting Optimal Trim Configuration of Marine Vessels with respect to Fuel Usage
A 60 ECTS credit units Master's thesis

Faculty of Industrial Engineering, Mechanical Engineering and Computer Science
School of Engineering and Natural Sciences
University of Iceland
Hjardarhaga 2-6
107 Reykjavik, Iceland
Telephone + 354 525 4000

Print in Háskólaprent
Reykjavik, Iceland 2009

Abstract

High fuel prices and environmental concerns are compelling shipping companies to consider how the fuel efficiency of vessels can be improved in order to reduce cost. Since the fuel cost is by far the largest portion of the operating cost of a vessel, a fractional savings in fuel usage can result in considerable savings in operational costs. Furthermore, fuel savings have environmental benefits in the reduction of greenhouse gas emissions.

Many operational optimizations for marine vessels concentrate on minimizing the fuel consumption by optimizing the vessel speed. However, during a typical cruise, the captain of the ship must meet a predefined schedule which limits the scope for speed optimizations.

Trim and displacement i.e. the difference between the draft at the bow and the stern and, the volume of sea displaced by the ship are, alternatively, controlled parameters worthy of attention with respect to fuel usage while the ship is cruising. Both can be controlled by arrangement of ballast. It has been shown that the power performance of vessels vary with different trim configurations. Often, the trim configuration is such that it is not operated at the optimal efficiency level. A substantial amount of money could be saved by trimming the vessel correctly.

In this thesis, black box models are used to predict how the power consumption depends on the trim given various input parameters. The goal is to find the lowest power consumption with respect to the trim.

The investigation is based on empirical data sampled at a passenger and freight vessel with a cruising schedule based in the North-Atlantic Ocean. The difficulty with such data, sampled under normal operation, is that the range of the numerous parameter values can be quite narrow, which may in turn limit the predictive accuracy of a regression model. Careful attention must also be given to the preprocessing of said data. It is shown how to deal with these aspects resulting in prediction models of trim configuration with potential fuel usage savings.

The method presented here can likewise be applied to other types of vessels such as; cruise liners, cargo ships and tank ships. The aim is to make such models part of an overall energy management system on board marine vessels.

Keywords: Black-Box Modelling, Energy Management, Functional Learning

Ágrip á íslensku

Skipafyrirtæki eru í síauknum mæli að leitast við að lækka rekstrarkostnað skipa með því að ná sem hagstæðustu nýtingu á olíu við keyrslu þeirra. Þar sem olían er langstærsti kostnaðarliðurinn mundi umtalsverður sparnaður fást með betri nýtingu á henni. Aukinheldur, hefur hagstæðari olíunýting í för með sér minni áhrif á umhverfið með minnkandi útblæstri.

Oft er einblínt á hraðann eða siglingarleiðir þegar hagræðing á rekstri skipa ber á góma. En þær hagræðingar eru þeim takmörkunum háðar að skipstjórinn þarf að fylgja áætlun sem gefur þröngar tímaskorður. Stafnhalli og særými, þ.e. munurinn á djúpristu stefnis og skuts og rúmmál vatns sem skipið ryður frá sér, eru á hinn bóginn, breytilegar stærðir sem vert er að gefa gaum á meðan siglingu stendur. En þeim má stjórna með því að stilla kjölfestuvatn á skipum. Þar sem sýnt hefur verið fram á að olíunýting skipa er mismunandi með mismunandi stillingum á stafnhalla mætti spara verulegar fjárhæðir með því að stilla stafnhallann á þeim þannig að hagstæðasta olíunýting náist.

Svartkassalíkön eru notuð í þessari ritgerð til að spá fyrir um hvernig ásafl á framdrift skips er háð stafnhallanum við gefnar aðstæður. Markmiðið er að finna lægsta aflið miðað við stafnhallann. Rannsóknin byggir á gögnum sem hafa verið söfnuð á farþegaskipi sem siglir samkvæmt áætlun í Norður-Atlantshafi. Huga þarf sérstaklega að forvinnslu gagna og einnig þeim takmörkunum sem svið sumra breytistærða hafa á spáhæfni aðhvarfslíkana. En þau geta verið þröng þegar gögnum er safnað við eðlilegar aðstæður. Sýnt verður hvernig unnið er á þessum atriðum þannig að hægt verði að búa til spálíkön fyrir stafnhalla sem geta mögulega leitt til sparnaðar á olíu.

Aðferðirnar geta einnig verið notaðar á aðrar gerðir skipa svo sem skemmtiferðaskip, flutningaskip og tankskip. Markmiðið er að nota þær í alhliða orkustjórnun skipa.

Efnisorð: Svartkassalíkön, Orkustjórnun, Lærdómsvélar

Acknowledgements

I have been given the opportunity to be under the guidance of Professor Sven Þ. Sigurðsson and Professor Tómas P. Rúnarsson in my master's program. I want to express my sincere gratitude to them for their contribution, constructive criticism and encouragement during my theoretical studies. Furthermore, I would like to thank Marorka and my coworkers there, Dr. Jón Ágúst Þorsteinsson, Stefán Sturla Gunnsteinsson, Kristmundur Guðmundsson, Grímur Jónsson, Rafn Magnús Jónsson, Kristinn Aspelund, Ari Vésteinsson, Gunnar Stefánsson and the rest of the staff for their help and contribution. Finally, I would like to thank Marion Scobie for improving the text in numerous ways.

Stefán Pétursson

Contents

Chapter 1

Introduction

High fuel prices and environmental concerns are compelling shipping companies to consider how the fuel efficiency of vessels can be improved in order to reduce cost. Since the fuel cost is by far the largest portion of the operating cost of a vessel[1], a fractional savings in fuel usage can result in considerable savings in overall operational costs. Furthermore, fuel savings have environmental benefits in the reduction of greenhouse gas emissions. Likewise, globally, nations and corporations alike are under pressure to reduce CO_2 emissions due to its proposed greenhouse effect.

In this thesis, black-box models are utilized to describe the relationship between a vessels' fuel consumption and its trim, in order to find the trim configuration that generates peak fuel efficiency. This chapter commences with some background information and the motivation behind performing this investigation. The objective is then presented, followed by the outline of this thesis.

1.1 Background and Motivation

Designers and manufacturers aim to produces vessels and propulsion systems which operate as efficiently as possible. Yet, when deployed for commercial usage, the systems will often not run at their optimal efficiency level. Thus, the possibility of fuel efficiency enhancements is a viable option for ship owners while operating vessels.

However, many operational optimizations for marine vessels concentrate on minimizing the fuel consumption by optimizing the vessel speed[2] or, by finding the optimal route[3]. Nevertheless, during a typical cruise, the captain of the ship must meet predefined schedules which limit the scope for speed optimizations. Yet, it has been shown that the power performance of vessels vary significantly with different trim configurations [4, 5, 6, 7]. Configuring the trim of ships in harbor does not suffice due to the known *squat* effect [8]; the phenomenon of a vessel's increased immersion and trim

when underway in water, as compared to calm water floating conditions. Often, the ships' trim configuration is such that it is not operated at the optimal efficiency level while the vessel is cruising. Figure 1.1 illustrates how the total fuel consumption for a vessel is divided. Three quarters of the fuel consumption is spent on the propulsion system, while the remaining quarter is spent on other operational machinery. Since such a significant portion is spent on the propulsion system, trimming the vessel correctly during a voyage could potentially save considerable amounts of money.

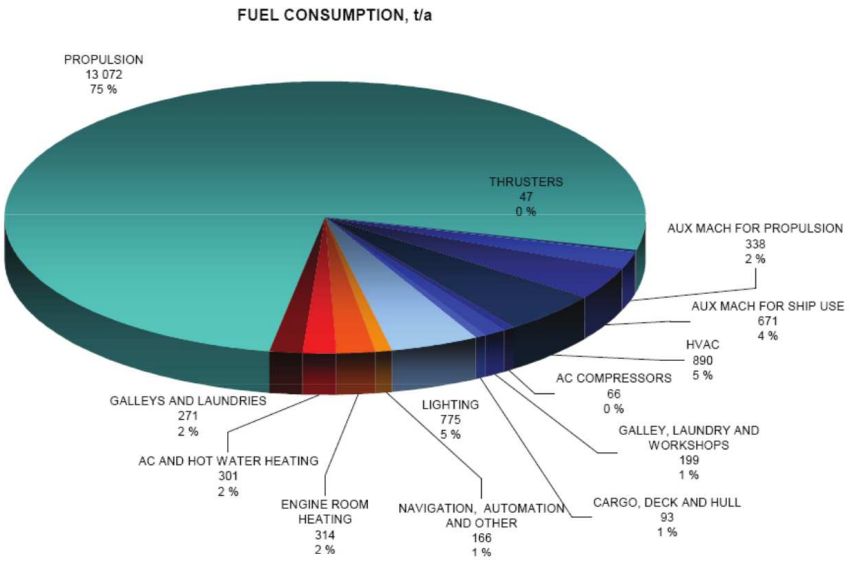

Figure 1.1: This figure illustrates how the total fuel consumption is divided. Three quarters of the fuel is spent on the propulsion system while the remaining quarter is spent on other operational machines.[9].

Many methods have been devised to enhance the fuel efficiency of vessels. Some of which are applied during the design phase when the hull of vessels and the propulsion systems are improved[10]. Others focus on energy efficiency by simulating the energy system for potential improvements[11], while some concentrate on the operational optimization of vessels[2]. A thorough research has been conducted on a semi-submersible heavy lift vessel with the object of assessing the feasibility of using models created with regression analysis in conjunction with physical laws, to optimize fuel consumption[5].

An Energy-System Design Toolbox (EDT)[12, 11], has been developed at Marorka[1] for simulating the energy systems of vessels for overall energy system optimization. It is utilized by means of Maren, which is a comprehensive energy management system developed at Marorka for real-time decision

[1]See `http://www.marorka.com`

support during vessel operation.

These type of models, i.e. those that are based on physical laws and prior knowledge, are often called white-box models. They describe how the fuel is transformed into thrust through the propellers, in order to overcome the resistance to the motion with the result of maintaining constant speed[13, 14]. They are quite effective but they lack the capacity to accurately include many aspects of the resistance such as the effects of wave [15], wind [16] and trim. Even though there are not many models that can accurately take the trim and displacement into account[1], thorough research projects exist that have allowed for them with positive results[5].

Alternatively, learning machines, also known as black-box models such as support vector regression and k nearest neighbor are quite capable of including input parameters that are difficult or even impossible to include in a physical model, such as ocean wave and wind. Artificial neural networks, for example, have proven to be feasible in predicting the power usage of vessels[17].

The main differences between these types of models are:

White box models are created from physical laws and prior knowledge. They tend to be good at extrapolating beyond operational data range but can be very poor at including all aspects of the physical reality.

Black-box models are created empirically from data points. They form a function by describing a relationship between input and output data. They are suitable when the system is not entirely understood but they have limited extrapolation capabilities.

A hybrid of those two models, often referred to as a grey box modelling, has been studied with promising results[18].

Black-box models will be utilized in this thesis, since they can often describe the relationship between input parameters and output data which can be difficult to do with a physical model.

1.2 Objective and Contribution

The objective of this thesis is to use a data set, sampled on a passenger ship, to generate black-box models that will be used to predict power requirements for various configurations of trim, given diverse external and operational conditions. While the main objective is to find the trim configuration that yields the least fuel consumption, the aim is to create a simulation model functional in a decision support system for potential fuel usage savings.

The contribution of this thesis is the methodology and evaluation concerning the viability of utilizing black-box models to predict the power consumption for various trim values, in an attempt to optimize the trim configuration in regards to fuel usage.

A typical result is depicted in figure 1.2; the ship is trimmed at 1 meter but the optimal fuel usage, with respect to the trim configuration, is considered to be when the ship is trimmed at -0.5 meters, given that the other input parameters are not altered.

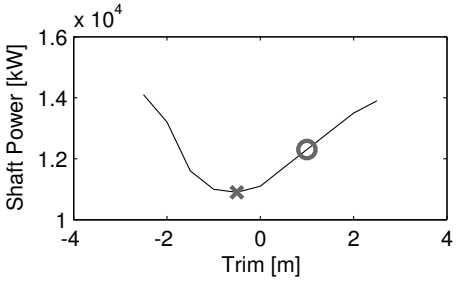

Figure 1.2: An ideal result where the point marked with `O` is where the vessel is currently trimmed at (1.0m) and the optimal trim suggestion is at the point marked with `X` (-0.5m).

1.3 Outline

Chapter 2 introduces the propulsion system and the resistance of the vessel which must be overcome in order to move it at a constant speed. This chapter serves as an introduction to some of the input and output parameters that will be used in the models.
The data set and its characteristics are described in Chapter 3 followed by how it is preprocessed, in Chapter 4.
Chapter 5 includes a short introduction to the black-box models considered in this thesis.
Chapter 6 coalesce the previous chapters where black-box models are applied to the data. Results from an experimental study on a passenger and freight vessel Norröna, are presented and, the chapter concludes with some remarks on the feasibility of this approach.
Finally, conclusions and further work are presented in chapter 7.

Chapter 2

Resistance of Vessels

In this thesis, the focus is on the relationship between the fuel consumption and trim of a vessel. The fuel consumption relates to the shaft power of the vessel that, by means of the propellers, provides the thrust needed to move the vessel at a given speed by overcoming any resistance to movement. Changes in the trim of the vessel affect this resistance but since one cannot readily isolate this effect, all the factors affecting the resistance have to be considered in a model that adjoin the fuel consumption to the trim. In this chapter, the relationship between fuel consumption and shaft power will be briefly described, which will be followed by a review of the main factors affecting the resistance. The chapter will be concluded by showing which factors are taken into account when constructing a black-box model allowing for the relationship between fuel consumption and trim.

2.1 Propulsion System

The thrust delivered by the propeller must be in equilibrium with the total resistance of the ship. The fuel is transformed into thrust through the propellers, overcoming the resistance to the motion, with the result of moving the vessel at a designated speed.

Figure 2.1 illustrates how the power is propagated through the propulsion system. The primary source of the propeller power is the diesel engine where the fuel is transformed into brake power, P_B. The relationship between the fuel consumption, the specific fuel consumption (SFC), and the brake power is

$$\text{Fuel consumption} = \int P_B \cdot SFC(P_B)dt \tag{2.1}$$

Figure 2.2 illustrates the relationship between the specific fuel consumption and the engine load which is defined as $P_B/P_{B_{\max}}$ where $P_{B_{\max}}$ is the maximum power delivered by the engine. It is obtained by simulating Norröna's engine in Marorka's Energy Design Toolbox (EDT).

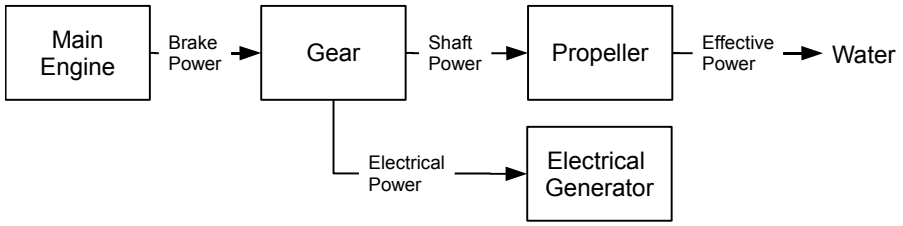

Figure 2.1: The propulsion system. The fuel is converted into break power which is transmitted to the propulsion shaft and the electrical generator. The shaft power is subsequently transformed, through the propellers, into thrust delivered to the water, otherwise known as effective power

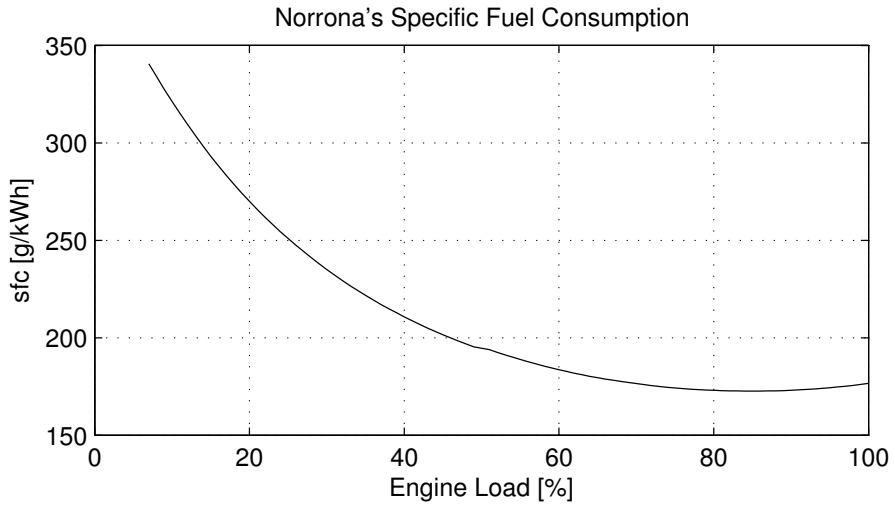

Figure 2.2: The relationship between Norröna's specific fuel consumption as a function of engine load, which is defined as $P_B/P_{B_{\max}}$ where $P_{B_{\max}}$ is the maximum power delivered by the engine, at a fixed rotational velocity.

The brake power, P_B, is transmitted to the propulsion shaft on the one hand and to the electrical generator on the other, through the gear:

$$P_B = \eta_B(P_S + P_{\text{el}}) \tag{2.2}$$

where P_S is the shaft power, P_{el} is the power transmitted to the electrical generator and η_B is the efficiency factor of the gear which is considered to be constant.
Subsequently, the shaft power is transmitted to the propellers

$$P_S = \eta_S P_D \tag{2.3}$$

where P_D is the power delivered to the propellers and η_S is the efficiency factor of the shaft which is considered to be constant.
The propeller power is transformed into thrust delivered to the water

$$P_E = \eta_P(pp, V, n)P_D(V) \tag{2.4}$$

where η_P is the efficiency factor of the propeller which is dependent on the propeller pitch, pp, the speed, V, and the rotational velocity of the shaft,n. The effective power of the vessel is P_E, i.e. the power necessary to move the ship through the water at speed V.

Often, the shaft has a constant rotational speed. The speed of the vessel is then controlled by changing the pitch of the propeller. Consequently, the propeller pitch is part of an operational condition that can be controlled. The relationship between the effective power, P_E, the various resistance forces, R_i, the propeller pitch, pp, and the speed of the vessel, V, is governed by the following equation[19, 7]

$$P_E(pp, V) = V \sum_i R_i(V) \tag{2.5}$$

indicating that many of the resistance forces also depend on the speed.
By combining equations 2.3 and 2.4, equation 2.5 can be restated as follows

$$P_S = \frac{V \sum_i R_i(V)}{\eta_S \eta_P(pp, V)} \tag{2.6}$$

Thus, the shaft power can be considered to be the power that overcomes the total resistance.

2.2 Vessel's Resistance

The total resistance to the movement of the vessel can be partitioned into resistance components as follows:

$$R_{\text{total}} = R_{\text{frictional}} + R_{\text{wave}} + R_{\text{wind}} \tag{2.7}$$

Frictional resistance is the resistance of the vessel's hull under the water line, *wave* resistance is the combined resistance from waves generated from external conditions and the waves produced from the vessel, and *wind* resistance is the resistance made by the wind on the hull above the water line. Figure 2.3 illustrates the three main components affecting the total resistance.

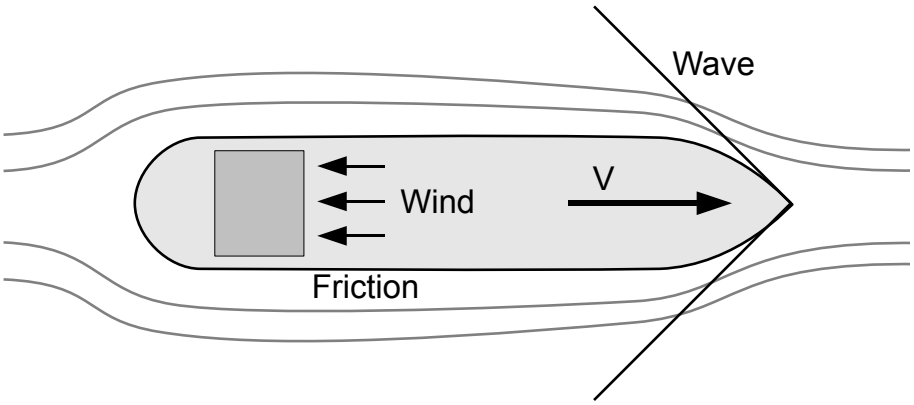

Figure 2.3: The three main resistance factors contributing to the total resistance. Frictional resistance is the hull's resistance below the water line, wind resistance is the hull's resistance above the water line and wave resistance is the resistance from the ocean surface and the waves produced by the vessel.

Each of these component resistances will be discussed in more detail in the following subsections.

2.2.1 Frictional Resistance

The frictional resistance is the most significant contributor (45-90%[19]) to total resistance and it increases at a rate that is close to the square of the vessel's speed. It is likewise subjected to how much of the hull is below the water line as well as the shape of the hull. With this in mind, and the fact that the shape of the hull is not symmetrical, the trim and displacement of the vessel also have influence on the frictional resistance since the area of the wetted surface changes with different configurations of trim and displacement. Furthermore, the surface of the hull below water line will be subjected to the growth of algae and weed which amplifies the resistance considerably with time.

Thus, the frictional resistance can be split further into the *hull* resistance, the *fouling* resistance and the *trim* and *displacement* resistance, each of which will be discussed in the following paragraphs.

Hull Resistance

The dynamic pressure of water with density, ρ, induces a resistance on the hull based on Bernoulli's law

$$R_{\text{hull}} = \tfrac{1}{2} C \rho V^2 A_{\text{hull}}$$

where V is the speed, A_{hull} is the area of the hull below the water line and C is a dimensionless resistance coefficient. The frictional resistance is, for that reason, highly dependent on the speed of the vessel.

Fouling Resistance

Fouling of a ship's hull is a biological process induced by the growth of algae, weed and other marine life forms. Sailing routes have a great impact on fouling since some areas have higher fouling effects than others, both seasonally and in regards to localizability. Figure 2.4 depicts how required propulsion power increases over 30% in order to maintain the same speed 2 years from last docking[1]. The resistance caused by fouling may become

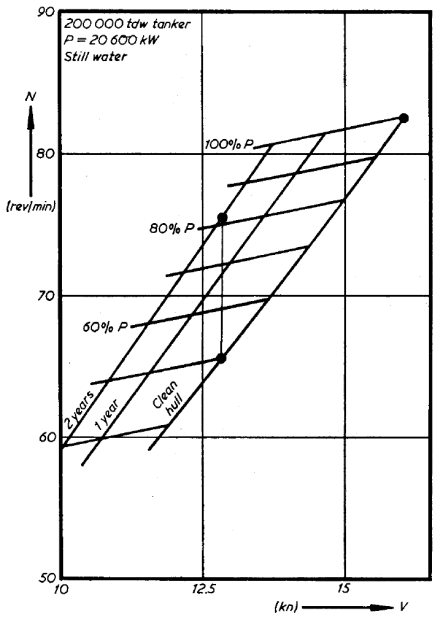

Figure 2.4: The relationship between propulsion power and speed for a 200000 tdw tanker with a fixed propeller, for a clean hull and 1 and 2 years after cleaning. Over 30% increase of propulsion power is required to maintain the same speed 2 years from last docking[1].

25-50% of the total resistance throughout the lifetime of a ship[19]. Fouling induces a condition that is difficult to control. It can be temporarily avoided

with the use of anti-fouling hull paints but the vessel must still be cleaned on a regular basis in a designated dock yard, as fouling increases considerably with time. Figure 2.5 illustrates how the fouling affects the resistance as a function of time.

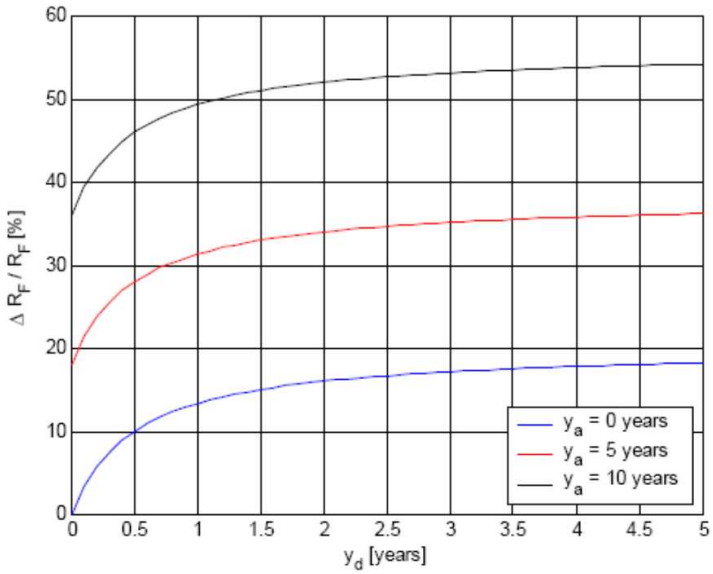

Figure 2.5: The figure shows how the percentage relative fouling of a vessel changes with time from docking, y_d, dependent on the age of the ship, y_a[5].

Trim and Displacement

The displacement of a vessel is equal to the mass of water displaced by the ship and, trim is defined as the difference between the draught of the hull at the bow and at the stern as seen in figure 2.6. They are, in particular, part of an operational condition that can be controlled by relocation of the vessel's ballast water.

Researches have shown significant variability of the delivered power performance with different displacement and trim conditions[4, 5, 6, 19]. Likewise, there is as relationship between hull form, due to trim and displacement, and power consumption. With different trim configurations the shape of the hull below the water line changes, affecting the frictional resistance.

Figure 2.7 illustrates how different displacement configurations affect the fuel consumption while the trim is held constant at zero. The fuel consumption increases significantly in concurrence with increases with the draught of the ship.

Figure 2.8 depicts how the trim adjustments affect the fuel consumption while the displacement is held constant by relocating the ballast water. There

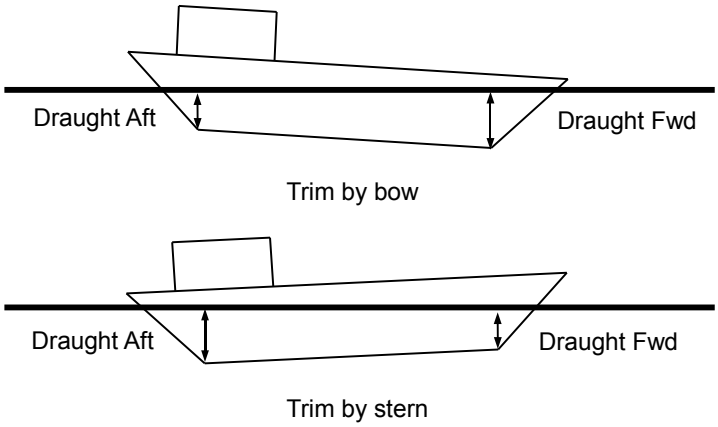

Figure 2.6: Different trim configurations. Above: trim by bow. Below: trim by stern.

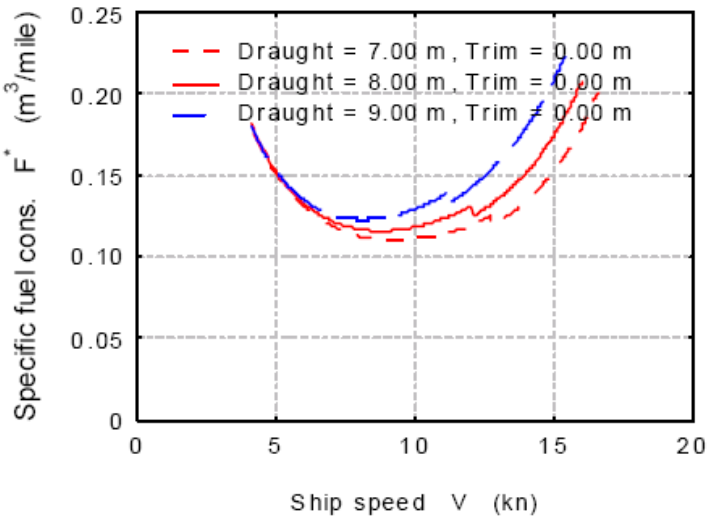

Figure 2.7: The relationship between speed, V, and specific fuel consumption, F, for different draught, with zero trim. The fuel consumption increases as the draught increases[5].

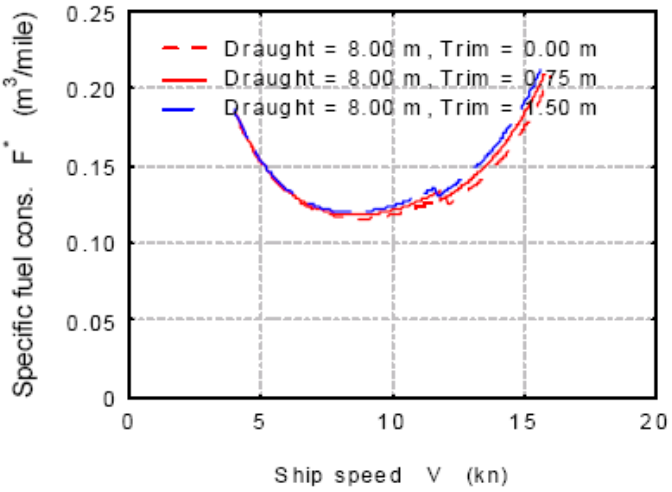

Figure 2.8: The relationship between speed, V, and specific fuel consumption, F, for different configurations of trim, with draught at 8m. The fuel consumption varies slightly with different trim configuration[5].

is a slight increase of fuel consumption per mile with an increasing trim.

Other Resistance

There are other conditions that affect the frictional resistance that will not be discussed in detail in this thesis. Deterioration of the paint and erosion of the hull both affect the frictional resistance directly. Rough weather and inappropriate distribution of the cargo are also examples of operational conditions that have effect. Likewise, shallow waters have influence on the resistance as the displaced water under the ship will have greater difficulty in moving aft-wards[19].

2.2.2 Wind Resistance

The wind affects the hull above the water line and forms a resistance factor that represents up to 2-10% of the total resistance[19]. Wind is part of an external condition that cannot be controlled since wind resistance depends on the direction and the speed of the wind. Resistance is essentially proportional to the square of the ship's speed and proportional to the cross-sectional area of the ship above the water line. Finding a suitable model for predicting wind resistance can be a difficult task[1, 16, 7] as vessels come in all sizes and shapes e.g. cargo ships, tankers, cruise liners.

Steering Resistance

In order to maintain the heading at a beam wind, rudder angle is necessary to counteract the wind moment at any given time[1]. This will cause added resistance to the vessel. The correcting autopilot will cause the vessel to sail with yaw motions when cruising in waves. They will cause centrifugal forces of which the component, R_{ST}, in the longitudinal direction results in added resistance[1] (see figure 2.9).

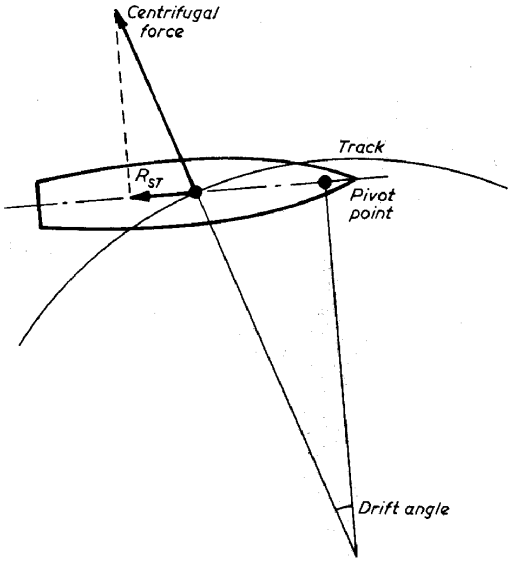

Figure 2.9: The steering resistance, R_{ST}, is caused by the centrifugal force when the vessel sails with yaw motions due to waves and correcting autopilot.[1].

2.2.3 Wave Resistance

The sea surface is assumed to be the result of the superposition of many simple harmonic waves, each with its own amplitude, frequency and direction of wave travel[1]. Ocean waves, in particular, can be split into two main wave types:

Sea Sea waves are driven by the local wind field. They are short-crested with lengths of the crests only a few times the apparent wave length.

Swell Swell waves are generated out of the local area, often created by storms many kilometers away. They are more regular and the crests are more rounded than those of a sea. Likewise, the frequency of the waves is much lower but the wave height is significantly higher.

Thus, waves are part of an external condition that cannot be controlled.

The wave resistance is comprised of waves created by the ship's propulsion through the water and breaking waves from the sea surface[13, 14]. Figure 2.10 illustrates how the mean wave resistance is added to the still water resistance in regular waves[20].

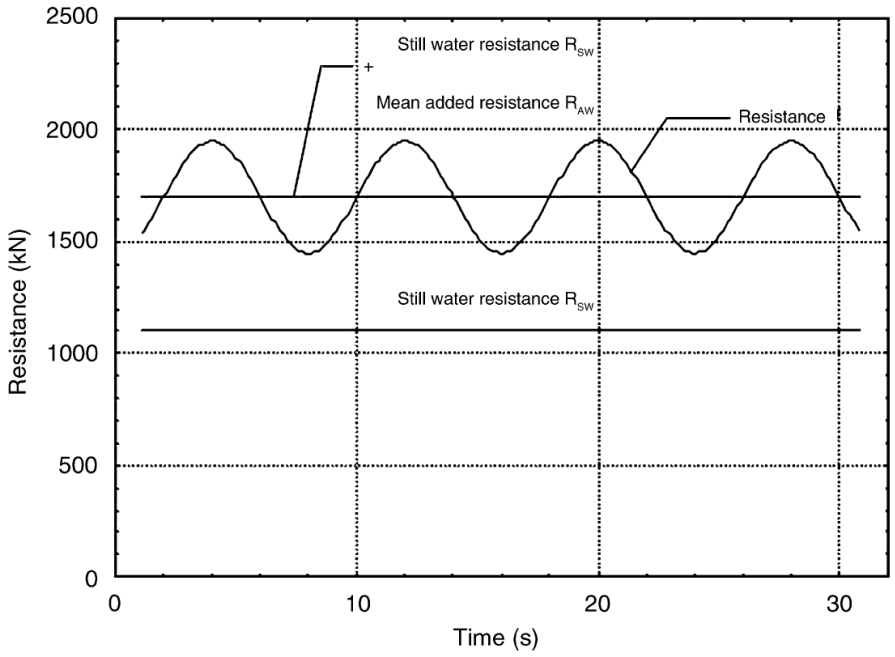

Figure 2.10: Figure showing the increase in actual and mean water resistance caused by regular waves[20].

In both situations the ship is transporting energy to the surrounding water and an added resistance has to be overcome to maintain the ship's speed[1]. Vertical ship motions have, in particular, the largest effect on the added wave resistance[1, 15, 20] where it can represent up to 5-45% of the total resistance[19].

The wave resistance is essentially proportional to the square of the speed. A speed barrier may be imposed since further increase of the ship's propulsion power will not result in a higher speed as most of the power will be converted into wave energy. Figure 2.11 depicts how the speed of the vessel drops considerably in head waves. It is complicated and difficult to predict the wave resistance of the vessel. Many models include some kind of a wave resistance prediction[15, 6, 1, 20], but their estimation is often inaccurate[1].

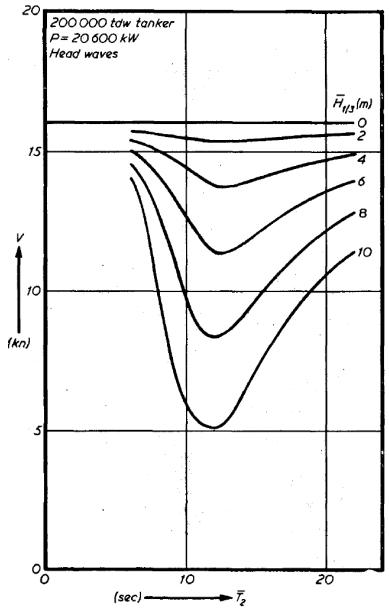

Figure 2.11: The relationship between speed and time for a 200000 tdw tanker when sailing in head waves. The lines show a speed reduction when sailing through a wave of height 2m, 4m, 6m, 8m and 10m[1].

2.2.4 Total Resistance

To sum up the previous sections, table 2.1 illustrates the proportion of each resistance factor to the total resistance

Resistance	% of Total Resistance
Friction	45-90
Wave	5-45
Wind	2-10

Table 2.1: The proportion of each resistance factor to the total resistance.

The total resistance is affected by operational and external conditions. The speed, trim and displacement are, for example, considered to be operational factors affecting the total resistance that can be controlled. Alternatively, external conditions such as wave and wind are resistance components that are not controllable.

2.3 Model Parameters

Most of the resistance factors presented in the previous section will be used in the construction of black-box models. The input parameters will be

Trim This is the main input parameter in the black-box models since the relationship between fuel consumption and different trim configurations is to be investigated.

Displacement The mean draught will be considered since it reflects the displacement to a certain degree.

Speed The speed of the vessel with respect to the water surface.

Wind The wind speed will be considered as well as the wind direction.

Wave The only wave resistance factor that will be considered is the vertical motion of the vessel as the data for other wave resistance factors are unavailable.

Propeller Pitch The propeller pitch will be applied since it is used to produce the thrust to move the vessel at a designated speed.

The fouling resistance will not be utilized since there are no measurements available and the data used for the black-box models cover a relatively short time interval. Likewise, the steering resistance will not be utilized either, since there is no data available measuring the yaw motion of the vessel.

The output parameter for the black-box models will be

Shaft Power The shaft power relates to the thrust needed to overcome the total resistance as indicated in equation 2.6 and can, unlike the effective power, be measured directly. The fuel consumption itself is not suitable as an output parameter since the main engine is also used to run the electrical shaft generator.

2.4 Summary

This chapter presents the general relationship between fuel consumption and shaft power on one hand and the various resistance factors on the other, which control the speed of the vessel. It provides a guide as to what factors should be taken into account when constructing a black model showing the dependence of fuel consumption on trim configuration.

Chapter 3

Data Set

The data obtained for this study was sampled on a passenger ship that has a cruising schedule in the North-Atlantic Ocean. This chapter starts by describing the operational and external data measurements that are considered to be related to the fuel consumption. They will be used as input and output parameters for black-box models. Subsequently, the characteristics of the data series are considered. They must be modified, in order to generate adequate black-box models.

3.1 The Vessel

Norröna[1] is a ferry/cruiser which has a sailing schedule between Iceland, The Faroe Islands and Denmark. Its length is approximately 160 m, the breadth is around 30 m and the mean draught is close to 6.5 m. Figure 3.1 is a picture of Norröna cruising in a calm water as well as a cross-section of the ferry.

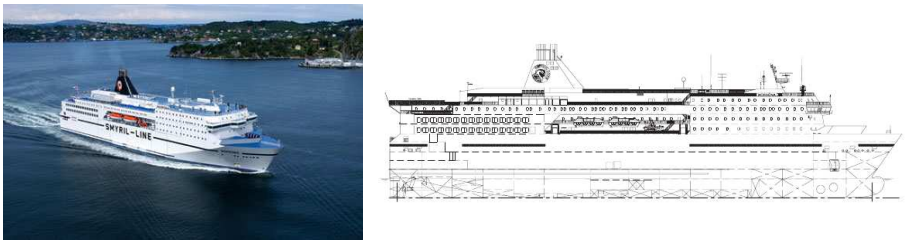

Figure 3.1: Norröna, a passenger and ferry ship, cruising in a calm water and a cross-section of the vessel[21].

Norröna has 4 main engines that have constant rotational velocity and two propellers to move the ship, as can be seen in figure 3.2. Since the engines' revolutions are constant the speed of the vessel is controlled by

[1]See `http://www.smyril-line.com`

changing the pitch of the propellers. Two electricity shaft generators are connected to each of the shafts to produce electricity whenever possible. Additionally, the vessel is installed with three auxiliary electricity generators to produce electricity if the electricity shaft generators are not in use.

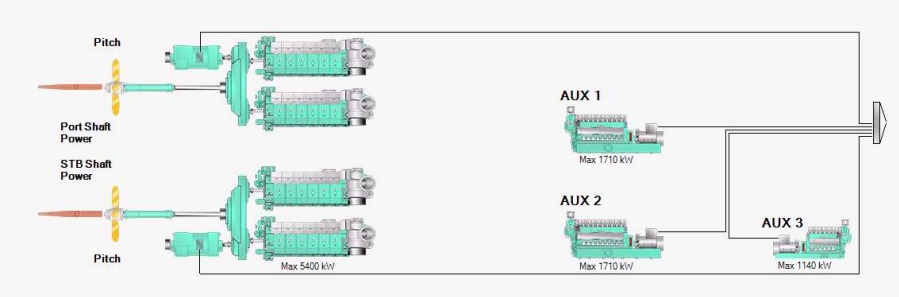

Figure 3.2: Norröna's machine layout taken from the Maren system on-board. The vessel has 4 main engines, two propellers, two electricity shaft generators and three auxiliary electricity generators.

An SMC[2] gyro scope sensor was installed specifically for this study, in order to measure the movement of the ship, as described in more detail below. Other measurements of the operational and environmental conditions of the vessel are sampled from previously installed meters.

3.2 Data Series

The output parameter of the models is the *shaft power* (kW) that the propellers deliver to the water through the propulsion shafts. The shaft power can be measured directly (figure 3.3) and is readily related to the fuel consumption via the specific fuel consumption of the engines and the power delivered to the electrical generators as shown in equations 2.1 and 2.2. The fuel consumption itself is not suitable as an output parameter since the main engine is also used to run the electrical shaft generator.

The main input parameter, *the trim* (m), is defined as the difference between the draught of the hull at the bow and at the stern. It can be calculated directly from the pitch of the hull shown in figure 3.6 (not to be confused with the propeller pitch) and since it is, in fact, the pitch that is measured (see figure 3.3), reference will be made to the pitch rather than the trim in the remainder of this thesis.

Apart from the shaft power and the pitch, numerous data series are sampled by the Maren[3] energy management system into a database at approximately 15 seconds intervals. Only a handful of them are considered

[2]See `http://www.shipmotion.se`
[3]See `http://www.marorka.com`

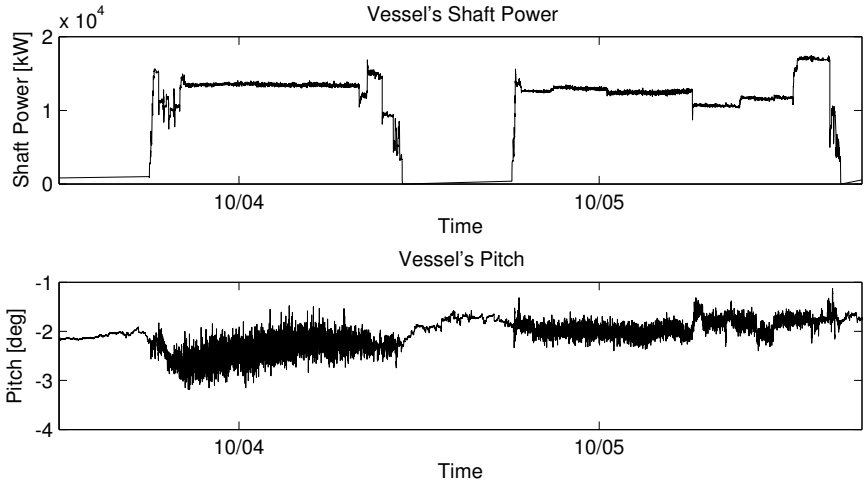

Figure 3.3: The shaft power consumption and pitch for two trips. These measurements are unfiltered.

to be connected to the modelling of the relation between shaft power and resistance to the movement of the vessel and, are thus used in this investigation. These parameters are comprised of operational measurements as well as external measurements.

The acquired data are measurements from various meters on-board the vessel; programmable logic controllers (PLC), systems using the NMEA[4] and OPC[5] protocols and, a SMC gyro motion sensor. It is assumed that all meters, excluding the gyroscope, are correctly set up and calibrated and their accuracy will not be specifically questioned apart from noise. The data domain consists of 26 trips, each lasting approximately 20-22 hours, which were made in the fall of 2007, a total of approximately 90000 data points.

3.2.1 Input Parameters

Input parameters to be used in the models are now described briefly:

Log Speed The log speed, measured in knots ([kn]), is the speed of the vessel in the water. The speed can be seen in figure 3.4 for two trips.

Wind Speed and Direction The wind speed, measured in knots ([kn]), is the speed of the wind relative to the ship. The wind direction is the direction, in degrees, of the wind relative to the head of the ship.

[4]National Marine Electronics Association
[5]OLE for Process Control

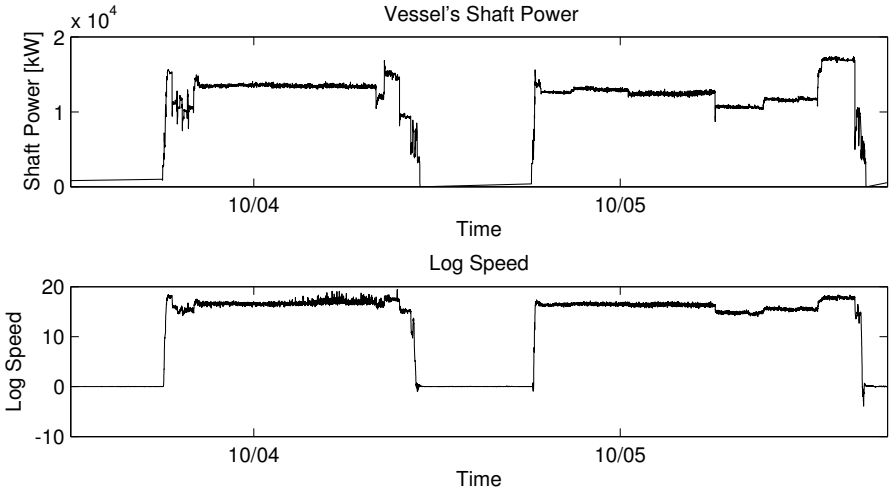

Figure 3.4: The log speed data series along with the shaft power series for two trips. These measurements are unfiltered.

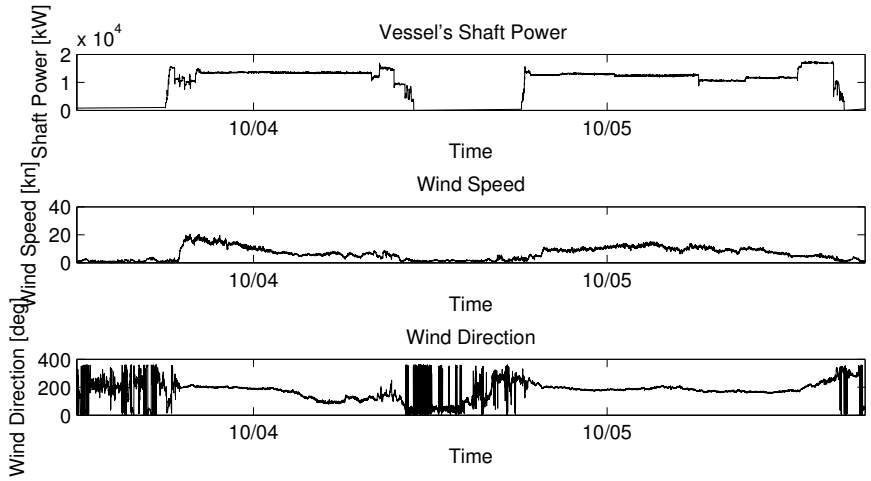

Figure 3.5: The shaft power consumption, wind speed and wind direction for two trips. These measurements are unfiltered.

Roll, Pitch and Wave The roll, pitch and heave of the ship are measured with the SMC gyro motion sensor which has the ability to measure the axial components along with the accelerometer component. The SMC device is installed in a location near the vessel's *centre of gravity* to ensure that the measurements will become as accurate as possible. In addition, it must be aligned so that the head of the gyroscope coincides with the head of the ship, for otherwise the roll and the pitch measurements will correlate.

As can be seen in figure 3.6 the *roll* is the measurement, in degrees, of the pitch along the Y-axis. The *pitch* refers to the pitch, in degrees, of the X-axis and the *heave* measures the acceleration of the ship up and down. From the heave measurements the estimate of the *wave* (figure 3.6) height is derived by calculating the highest absolute heave value between two consecutive zero crossings of the signal.

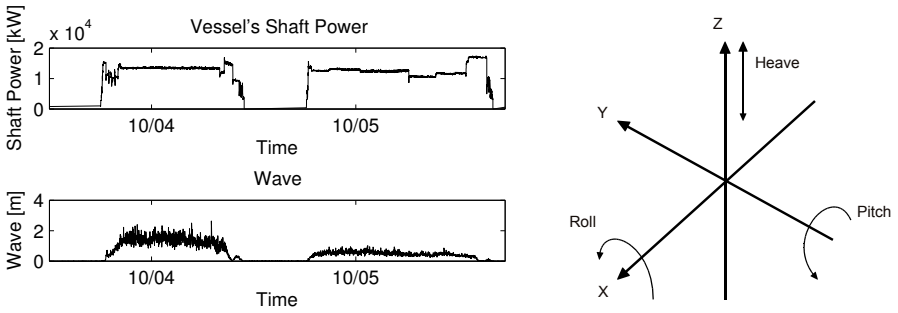

Figure 3.6: In the figure on the left, the wave is displayed for two trips. The illustration on the right shows how the roll, pitch and heave are measured by the gyroscope.

As previously mentioned, pitch is the main input parameter in this thesis as the focus of this thesis is on how shaft power varies with trim.

Mean Draught The *forward* and *aft* (m) measurements are the depth of the ship from the keel to the ocean surface - forward and aft respectively. Those measurements are not reliable under dynamic conditions since they are taken from sensors stationed forward and aft, which measure the pressure on the hull. However, they are quite steady when the ship is in harbour and are thus utilized to correct the roll and the pitch. They are also used to estimate the *draught* of the ship, which gives some information on the ship's displacement. Fuel consumption is affected by the vessel's displacement since the area of the hull below the surface directly affects the frictional surface.

Figure 3.7 illustrates the mean draught of the vessel. There seems to be correlation between the mean draught and the shaft power. This is due to the squat effect: the increased immersion of the vessel into the water with increased speed.

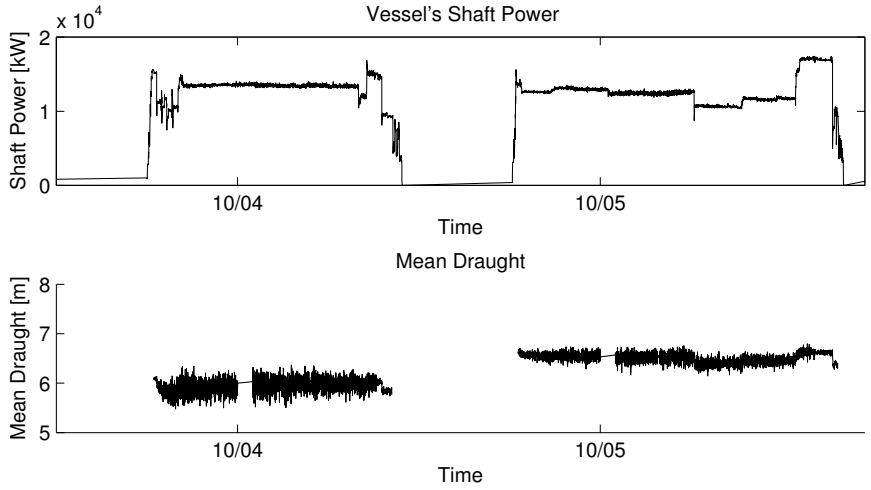

Figure 3.7: The mean draught of the vessel for two trips. There is a slight correlation between the shaft power and the mean draft due to the squat effect.

Propeller Pitch The pitch of the two propeller blades relative to the shaft are used to control the vessel's speed, and change during voyage. The propeller pitch is measured in whole numbers rendering a sawtooth time series, as can be seen in figure 3.8.

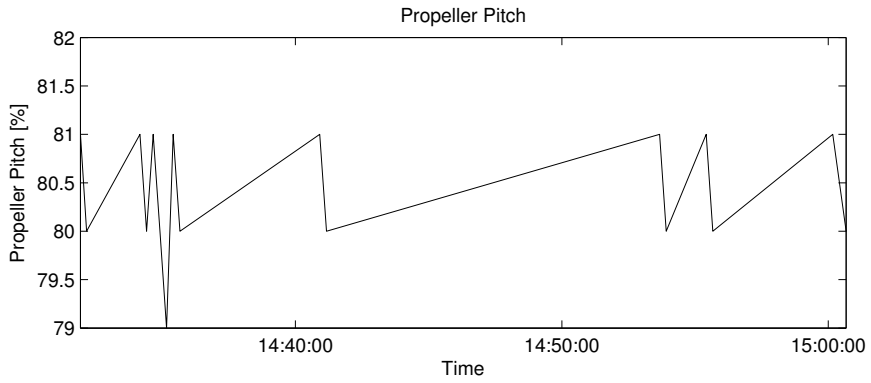

Figure 3.8: The measurements for the propeller pitch are a natural number rendering a sawtooth time series.

Thus the total of input parameters is 9.

3.3 Characteristics of the Data Set

In order to effectively apply a learning machine to the data it must be well formed and must therefore include synchronized measurements that correspond to reality as much as possible, while being devoid of corruption and outliers. In this study, this is not the case with the data series taken straight from the database. This section reviews those difficulties.

3.3.1 Data Sampling

The data series are *usually* sampled at 15 seconds intervals into a database but they are neither necessarily logged at a uniform time interval nor simultaneously. To save space, the database system writes one value for a sequence of data points if their measurements remain the same. Slowly changing measurements are specifically susceptible to this. Moreover, other data series can be corrupt in the sense that they are either frozen, characterized by measurement values remaining the same although conditions alter, or the measurements are simply not arriving to the database system. Such defective data, as well as slowly changing data, has to be detected and handled in a sensible way.

3.3.2 Weather Data

Figure 3.9 illustrates histograms for wind speed, wave height and pitch. Norröna's sailing schedule provides routes where there are occasional rough weather conditions, where wind speed can reach over 30 knots and wave height can reach over 10 meters. Rough weather conditions affect the mea-

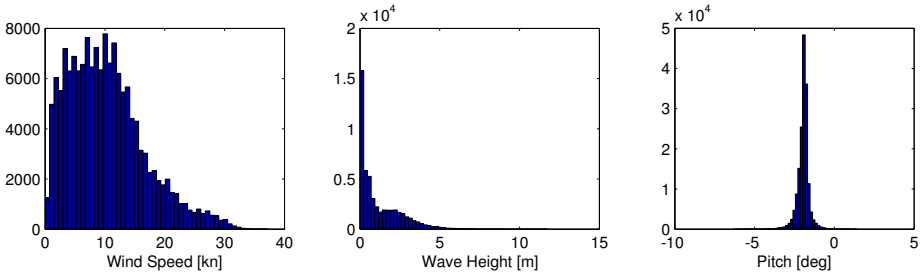

Figure 3.9: Histograms for wind speed, wave height and pitch. Norröna can occasionally hit rough weather conditions where the wind speed reaches over 30 knots and the wave height over 10 meters.

surements as they induce noise and extreme values. No attempt has been made to remove data segments corresponding to rough weather even though the application of optimal pitch configuration is not useful in these conditions.

3.3.3 Noise and Outliers

Measurements made by the meters are often susceptible to noise, specifically in rough weather conditions as can be seen in figure 4.10. It is important to filter this noise as well as defective outliers.

3.3.4 Gyroscope Installation

The gyroscope was installed such that the head of the device was misaligned with the head of the ship. This resulted in a high correlation between the roll and the pitch measurements, which had to be remedied.

3.3.5 Data Range

The range of the data must be broad in order to successfully generate an adequate black-box model that predicts the shaft power usage for various conditions. However, the difficulty with data sampled under normal operational conditions is, that the range of many of the parameter values can be quite narrow and may in turn limit the predictive accuracy of a regression model. See for example the histogram of the pitch in figure 3.9.

Furthermore, in this study, the focus is on how the shaft power changes with pitch while other input parameter values affecting the resistance remain fixed. Ideally, the data should be obtained from controlled experiments where the pitch is the only variable parameter. Clearly, this will not be the case when data is collected under operational conditions. Figure 3.10 illustrates this problem. The dots correspond to available data while the estimate is on data values along straight lines parallel to the pitch axis.

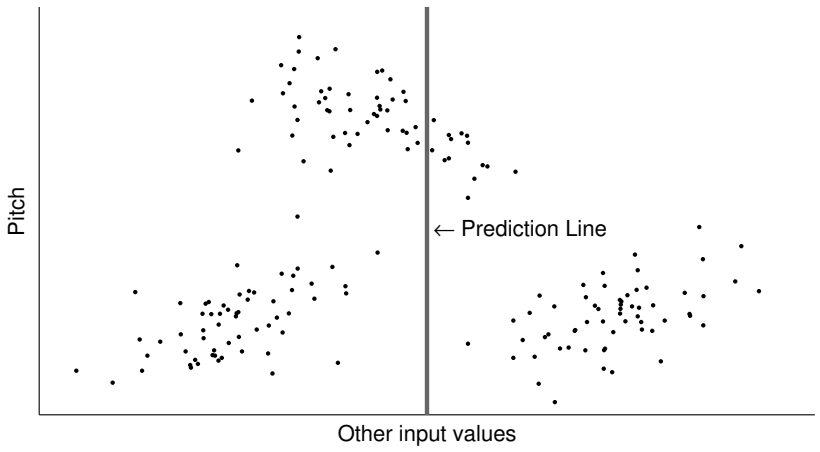

Figure 3.10: The distribution of the data is nonuniform making it difficult to predict how the shaft power changes with pitch, while other input values remain fixed.

3.4 Summary

This chapter describes the input and output parameters that will be used to generate the black-box models in subsequent chapters. The data series are measurements of both operational and external conditions believed to have the most influence on the vessel's shaft power. However, they are not without defects, which must be overcome in order to successfully generate the models.

Chapter 4

Data Preprocessing

The data series sampled from the vessel must be well formed, i.e. synchronized and corresponding to reality as much as possible in order to generate adequate black-box models. Due to the complications described in the previous chapter some preprocessing must be performed on the data in order to achieve this.

This chapter describes which actions are taken in order to generate a well formed data series. These include removing data segments, patching gaps in data, synchronizing the series in time, correcting data values, noise filtering and, removing outliers.

4.1 Data Pruning

Some sections of the data must be removed manually, i.e. data series that are severely corrupted or are otherwise not desirable based on visual inspection. This applies, in particular, to series where data values seem to be frozen for too long.

4.1.1 Automatic Data Removal

Some data sections are not interesting in this problem and only introduce additional complexity if included. Data sections acquired while the ship is in harbour are removed since the most important component in terms of fuel savings is when the ship is sailing. The next paragraph details how the harbour data is removed.

Removing Harbour Data

The Maren system on-board the vessel saves the shaft's rpm values to the database. They can be used to detect when the ship is in harbour since those values are non-zero while the ship is cruising. Therefore, gaps over 30 minutes in the time series are considered to be the time when the ship

is in harbour. Based on the rpm data series, all data series are split into chunks, each corresponding to one trip. Trips lasting less than three hours are considered to occur when the vessel is in *pilot* within a port, i.e. in control of the harbour authority, and are thus removed.

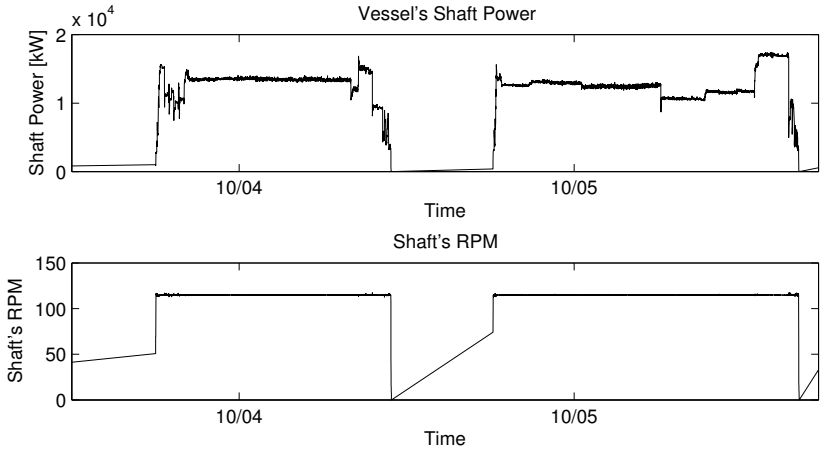

Figure 4.1: The shaft's rpm data series with the shaft power for two trips. The RPM measurements, which exist only when the vessel is cruising, are used to detect when the ship is in harbour.

Figure 4.1 illustrates the engine's rpm while cruising.

Additionally, the data segments at the start and end of a journey, where the ship is accelerating, are removed since these are relatively short and thus do not play a significant role in overall sailings. The following paragraph describes in detail how they are removed.

Removing the endpoints of a journey

The data chunks created by the method in the previous paragraph still hold data corresponding to start and end of a journey. The log speed (see figure 3.4) is used to detect the endpoints for each chunk in the following way: first, the log speed is resampled to create a time series with a uniform time interval between consecutive data points. Then it is filtered with a high order Equiripple Lowpass filter with a cut off frequency 1/400. The result is a noiseless data series which can be used in a simple *peak detection* algorithm: it finds those points where the derivative is zero. Figure 4.2 illustrates numerous peaks in a journey. The start of a journey is defined to be when the first peak value above 14 is detected (marked with a big circle in figure 4.2). Likewise, the last peak above 14 is considered to be the end of a journey. All data series are subsequently synchronized with intervals defined by these peaks values.

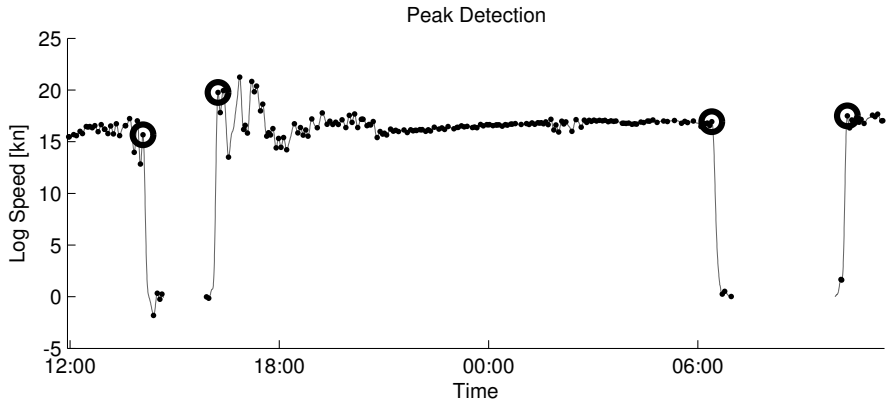

Figure 4.2: Peaks detected in a journey. The big circles represents the start and the end of the journey.

The log speed series was preferred to the shaft power data since the nature of the former was considered to be better suited for this task.

4.2 Data Patching

Some series change slowly over time, where it is normal to have recurrent consecutive values. Since the data points are not written to the database they must be generated to conform to other data series. Figure 4.3 illustrates how data points, for the propeller pitch measurements, are generated in between two consecutive points by assigning them with a value of the older point.

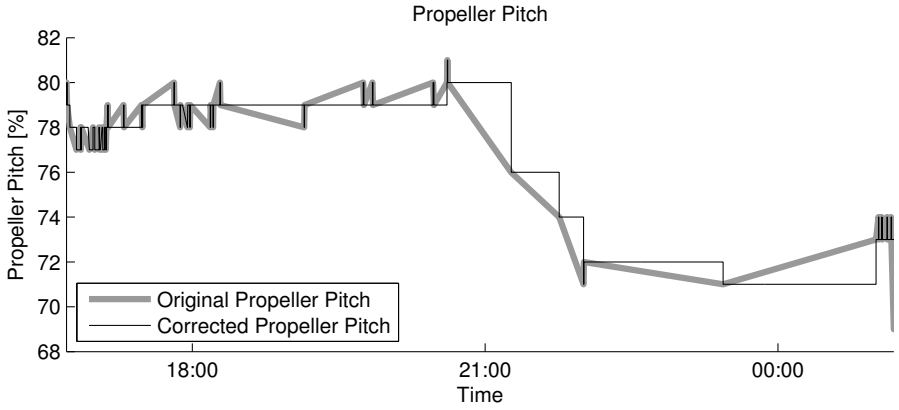

Figure 4.3: Data points are inserted in between two consecutive propeller pitch measurements with a value from the older point.

In cases, where measurements have not arrived, a linear interpolation is applied to "patch" the data series with data samples if the time gap is not too long. Gaps over 30 minutes are not patched as the condition of the ship might have changed too much for a simple linear interpolation correction.

None of the data series, where the value is rapidly changing, contain gaps that are too large to be patched with a linear interpolation. Gaps in those series rarely exceed 30 seconds.

4.2.1 Data Synchronization

After all unnecessary data sections have been removed the remaining data series are still not synchronized in time or of equal length. In this section the aim is to create time series of equal length for all parameters in such a way that the times of corresponding data points coincide.

As mentioned above, all data series are broken down into data chunks corresponding to approximately one trip. The data series for a given trip are synchronized with each other by removing non-overlapping data sections (see figure 4.4). Subsequently, the data points within each chunk are synchronized in time with the *shaft power* series by creating data points with linear interpolation and removing other points where applicable. This creates time series with nonuniform time intervals between data points. Usual filters cannot operate on such data without some kind of resampling. This problem is addressed in section 4.4 below.

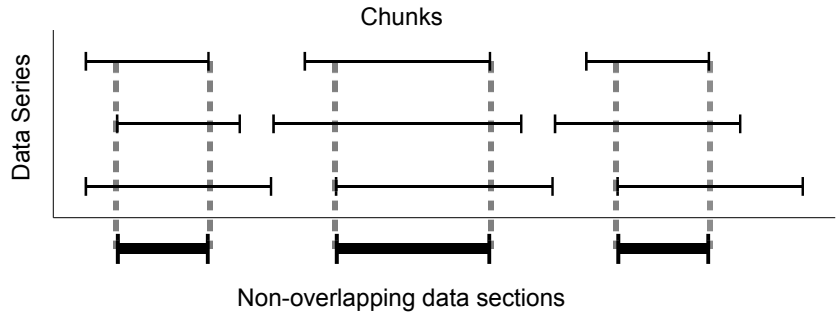

Figure 4.4: Data series are synchronized for each trip by removing non-overlapping data sections.

4.3 Data Correction

Some data series must be corrected before they can be used. The correction for the roll and the pitch series is described in the following section.

4.3.1 Roll and Pitch Corrections

The correlation between the pitch and the roll measurements should be zero since they are *orthogonal*. However, there is a correlation between them which indicates that the sensor was misaligned with the head of the ship. The pitch and the roll measurements from the gyroscope are corrected in this section to make them resemble the true pitch and roll measurements as much as possible.

Assume that the sensor is installed such that its alignment error is twofold. Figure 4.5 illustrates how the device is installed, at location O, with respect to the coordinates, XYZ, of the vessel where the pitch and the roll of the vessel is zero. The direction angle of the sensor is offset by a constant, θ, from the XZ-plane, i.e. the angle between OS and OP is θ. The pitch error, p_e, is the offset of the plane formed by OPS, which the device resides on, from the XY plane. That is, the angle between OP and OV is p_e. Implicitly, it is assumed that there is no roll error, i.e. that $PS||VD$, to simplify calculations.

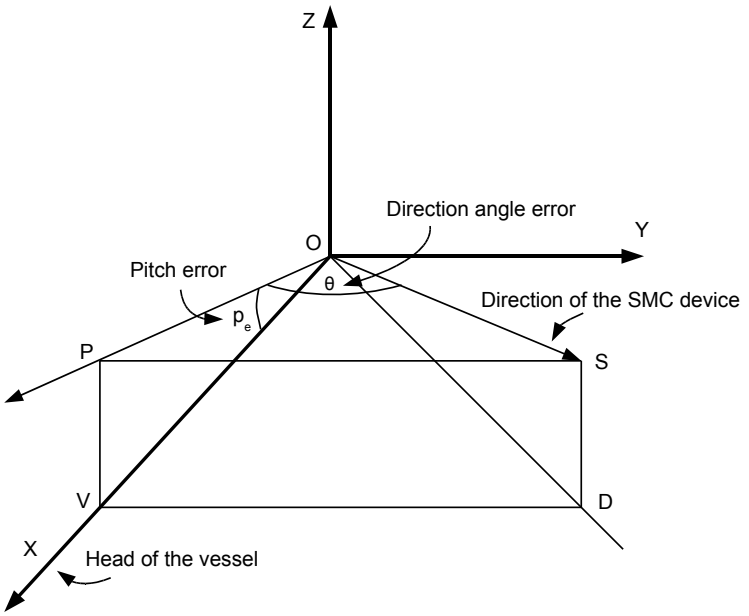

Figure 4.5: The device is installed, at location O, with respect to the coordinates, XYZ, of the vessel where the pitch and the roll of the vessel is zero. The direction angle of the sensor is offset by a constant, θ, from the XZ-plane, i.e. the angle between OS and OP is θ. The pitch error, p_e, is the offset of the plane formed by OPS, which the device resides on, from the XY plane. That is, the angle between OP and OV is p_e. Implicitly, it is assumed that there is no roll error, i.e. that $PS||VD$, to simplify calculations.

The correction of the roll and the pitch parameters are readily described according to the following definitions of the parameters used for this problem:

- p_e: The constant pitch error of the SMC gyroscope as described above (see figure 4.5). This constant is to be determined.
- θ: The direction angle error of the SMC gyroscope from the ship's heading as described above (see figure 4.5). This constant is to be determined.
- ϕ: The SMC's measurement of the pitch as described below (see figure 4.6).
- γ: The SMC's measurement of the roll as described below.
- f: Forward trim parameter value, measured from the forward trim sensor.
- a: Aft trim parameter value, measured from the aft trim sensor.
- L: The length between the forward and aft trim sensors.
- p: The true pitch of the vessel.
- r: The true roll of the vessel.

The true pitch of the vessel is calculated from the forward trim and the aft trim measurements, f and a, when the vessel is in harbour since they are reliable when the ship is not operated in dynamic conditions. The true pitch of the vessel is calculated from these measurements as follows

$$p = \sin^{-1}(\tfrac{f-a}{L}) \tag{4.1}$$

where the L is the length between the forward and aft sensors. L is not available for this problem and must be determined.

In order to correct the SMC's pitch and the roll measurements, ϕ and γ, a connection between them and the true pitch of the vessel, p, must be available.

To simplify calculations even more, the pitch error, p_e, is assumed to be on the XZ plane for all true roll values, r. This is a sensible approximation since the true roll values are close to zero. Then a connection between the SMC's pitch, ϕ, and the true pitch of the vessel, p, can be derived as can be seen in figure 4.6. The pitch of the vessel, i.e. the true pitch p, is the angle between OV and OA. The roll of the vessel, i.e. the true roll r, is the angle between PS and RS. The SMC's pitch measurement, ϕ, is the angle between OD and OS. If $|OS| = 1$, it follows that $|SD| = |RA| = \sin(\phi)$, $|OP| = \cos(\theta)$ and $|PR| = \sin(r)\sin(\theta)$. Then, by applying a simple trigonometry on the triangle $\triangle OPA$ the following ensues

$$\sin(p + p_e) = \frac{\sin(r)\sin(\theta) + \sin(\phi)}{\cos(\theta)} \tag{4.2}$$

The connection between the SMC's roll, γ, and the true pitch of the vessel

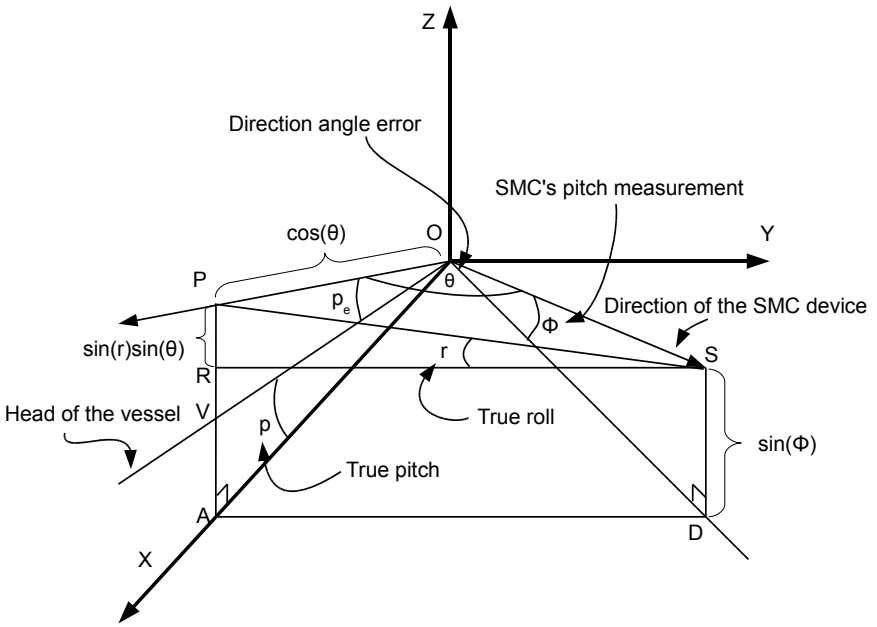

Figure 4.6: The connection between the SMC's pitch, ϕ, and the true pitch of the vessel. The pitch of the vessel, i.e. the true pitch p, is the angle between OV and OA. The roll of the vessel, i.e. the true roll r, is the angle between PS and RS. The SMC's pitch measurement, ϕ, is the angle between OD and OS. If $|OS| = 1$, it follows that $|SD| = |RA| = \sin(\phi)$, $|OP| = \cos(\theta)$ and $|PR| = \sin(r)\sin(\theta)$.

can be derived with similar reasons that will not be disclosed here:

$$\sin(p + p_e) = \frac{\sin(\gamma) - \sin(r)\cos(\theta)}{\sin(\theta)} \tag{4.3}$$

By isolating $\sin(r)$ in equations 4.2 and 4.3 and solving them together the following is derived

$$\sin(p + p_e) = \sin(\gamma)\sin(\theta) + \sin(\phi)\cos(\theta) \tag{4.4}$$

That is, a relationship between p, ϕ and γ.

In order to find p_e, θ and L the following minimization problem is solved with an unconstrained nonlinear optimization[1] for the data points from when the vessel was in harbour

$$\min_{\theta, p_e, L} ||p' - p''||$$

where

$$p'' := \sin^{-1}(\sin(\gamma)\sin(\theta) + \cos(\theta)\sin(\phi)) - p_e$$

is equation 4.4 where p has been isolated and renamed p'', and

$$p' := \sin^{-1}(\tfrac{f-a}{L})$$

is equation 4.1 with p' instead of p.

The results are $(p_e, \theta, L) = (-2.03, 14.5, 154)$ and the correlation changes from -0.33 to -0.11. The remaining correlation could stem from the fact that the SMC gyroscope isn't situated directly at the ship's centre of gravity, even though it is in close approximation.

Figure 4.7 illustrates how the roll and the pitch signals are correlated and how the correlation has diminished by applying the corrections to the data series.

Figure 4.8 depicts how the corrected SMC pitch compares with the pitch calculated from the forward and aft trim sensors. The RMS error between these data series is 0.1005.

4.4 Filtering the Data

Noise and outliers are undesirable in data series when it comes to employing them as inputs and outputs in black-box modelling. The learning machine could simply learn the noise, since the root mean square (RMS) error is used as the quality measure; rendering an unreliable model. Figure 4.9 illustrates two models where the one below has over-fitted the noisy data but has a lower RMS error value than the model on top.
When selecting the filter some considerations must be kept in mind:

[1] See `fminsearch` in Matlab

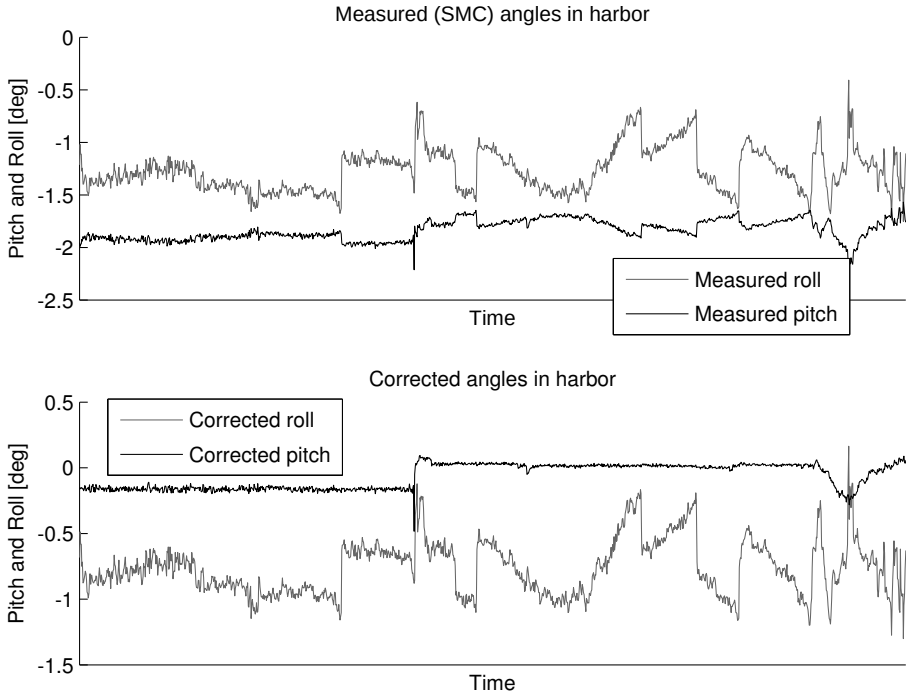

Figure 4.7: Above: a correlation between the roll and the pitch. Below: the correlation has been removed.

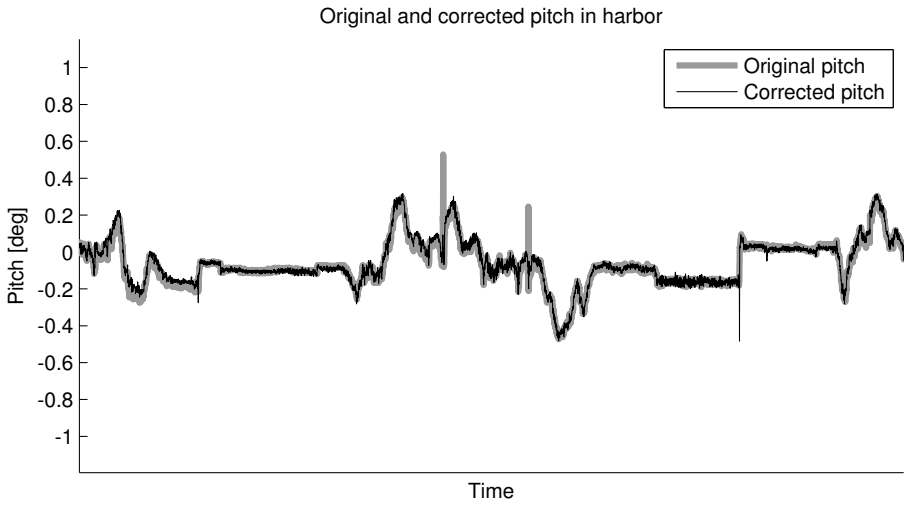

Figure 4.8: The vessel's true pitch calculated from the forward and aft trim sensors and the corrected SMC pitch.

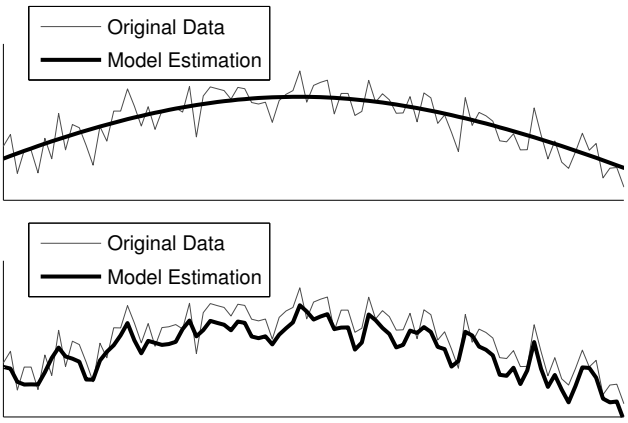

Figure 4.9: The model below has over-fitted the noisy data but has a lower RMS error value than the top model.

- The filter must be "as much" *on-line* as possible as this method is to be used on-board a ship for real time analysis. A delay of less than thirty minutes will be tolerable since the status of the ship will not change dramatically in that period on calm seas.
- The filter must handle data points that are not uniformly sampled.

A filter based on local linear regression, which is resistant to outliers and can handle data points that are not uniformly sampled[2], is applied to all data series. Figure 4.10 depicts how the noise is successfully removed and how the outlier is discarded without showing any sign of instability. The spike is obviously incorrect even though a few neighboring data points are contributing to the outlier.
The following paragraph describes in detail how the local linear regression filter, which is resistant to outliers, is implemented[22].

Local linear regression smoothing This method filters a data point over a span of n data points.

The weights for each data point within the span is calculated with:

$$w_i = \sqrt{\left(1 - \left|\frac{t - t_i}{d(t)}\right|^3\right)^3}, \quad i = 1, ..., n$$

where t is the time of the data point to be filtered. $t_j,\ j = 1, ..., n$, is the time of a data point j within the span. And

$$d(t) = \max_i(|x - x_i|)$$

[2]See `rloess` in Matlab

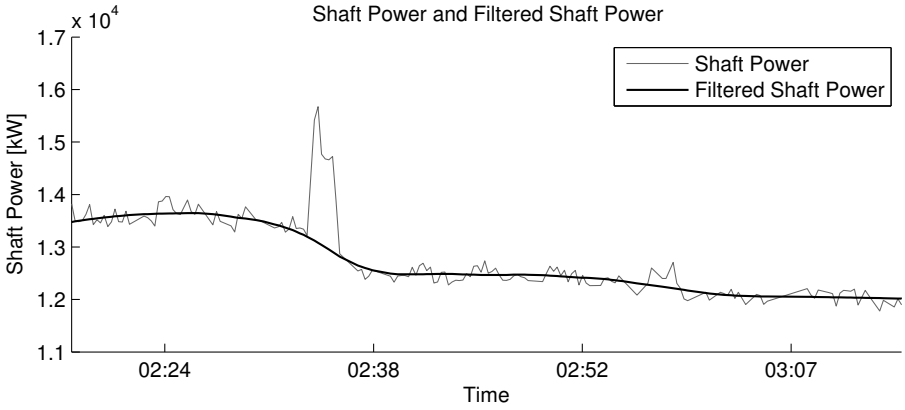

Figure 4.10: The shaft power series and a filtered shaft power series where the outlier has been discarded.

The data point which is to be filtered has the most weight while the weight of neighboring points decreases with distance from this point.

A weighted linear least squares regression using a quadratic function, $\beta_0 + \beta_1 t + \beta_2 t^2$ is performed by choosing $\hat{\beta} = [\beta_0 \ \beta_1 \ \beta_2]^{\mathrm{T}}$ such that

$$||\mathbf{W} \cdot (\mathbf{X}\hat{\beta} - y)||^2$$

is minimized. Here

$$\mathbf{X} = \begin{pmatrix} 1 & t_1 & t_1^2 \\ \vdots & \vdots & \\ 1 & t_n & t_n^2 \end{pmatrix}$$

$\mathbf{W}$ is the diagonal weight matrix and t_j, $j = 1, ..., n$, are the time stamps for the data points, $y_i, i = 1, ..., n$, in the span.

The filtered value is given by

$$y_{\mathsf{filtered}} = \mathbf{X_i} \cdot \hat{\beta}$$

where i is the index of the y value to be filtered and $\mathbf{X_i}$ is the i-th row in $\mathbf{X}$.

In order to remove the effect of the outliers the filtering is repeated five times with modified weights as follows

Calculate the residuals r_i, for each data point.

Let $r_{\mathrm{med}} := \mathrm{median}(\{r_i\}_{i=1}^n)$

Let $\rho_i := |r_i - r_{\mathrm{med}}|$, for $i = 1, \ldots, n$

Let $M := \text{median}(\{\rho_i\}_{i=1}^{n})$

Define a *modified weight* for each data point as $w_i R_i$ where w_i is the previous weight value and

$$R_i = \begin{cases} 1 - \left(\frac{\rho_i}{6M}\right)^2 & |\rho_i| < 6M \\ 0 & \text{otherwise} \end{cases}$$

Repeat the filtering calculations with these modified weights.

The final modified weight will be close to 1 if ρ_i is small; i.e. if the error is not significant. If, however, ρ_i is large (compared to other errors) then it will exceed a certain limit which will reduce the weight to zero.

This filter does not need a uniform sampling time and data points far away in time have no influence on the data point being filtered. A span of 50 data points was chosen for all the series as it was considered, by visual inspection, that the noise had been removed without removing vital information from the data series.

4.5 Summary

This chapter presents some preprocessing methods that are applied to the data series to be used to generate black-box models. The data series are pruned and synchronized such that the remaining data points correspond only to the vessel's journeys out of harbour, devoid of the acceleration that occurs at the start and the end of a trip. Moreover, they are patched, corrected and filtered which makes them suited for input and output parameters in learning machines.

Chapter 5

Black-box Models

This chapter describes the black-box models used in this study to simulate the shaft power. First a general description of functional learning is presented along with how model parameters are evaluated and how data is prepared. Support Vector Regression method is subsequently presented followed by a description on the k Nearest Neighbor model. The chapter then concludes with a brief description of Classification and Regression Trees, Bagging and Artificial Neural Networks.

Many types of problems cannot be solved by using classical programming techniques since the precise mathematical model is not at hand. This applies in particular when it proves difficult to relate the output to the inputs due to complexity or other factors such as noise, measurement inaccuracy, incorrect measurements or lack thereof. To remedy the situation, methods have been devised where the computer learns the relationship between input and output from given data.

5.1 Functional Learning

Given a set of data points, $(\mathbf{x}_i, y_i), i = 1, ..., n$, which is a relationship between input vector values $\mathbf{x}_i \in X$ and output values $y_i \in Y$, the aim is to find a target function

$$f : X \times \mathbb{R}^k \to Y; (\mathbf{x}, \mathbf{w}) \mapsto y$$

where $\mathbf{w} \in \mathbb{R}^k$ is a value of function parameters. The aim is to find a parameter value, $\hat{\mathbf{w}}$, such that $f(\mathbf{x}_i, \hat{\mathbf{w}}) \approx y_i,\ i = 1, ..., n$, but also such that $f(\mathbf{x}, \hat{\mathbf{w}})$ resembles reality for all $\mathbf{x} \in X$. I.e. $\hat{\mathbf{w}}$ is chosen so that a certain generalization error is minimized. The determination of $\hat{\mathbf{w}}$ is based on a given subset of the total data set, often referred to as the *training set*, while the validation of the resulting target function or model is based on the remaining subset, referred to as the *test set*.

The resulting target function, f, is chosen from a set of candidate functions forming a hypotheses space. The algorithm which takes the training

data as input and selects a hypothesis from the hypotheses space is referred to as the learning algorithm. Even though a hypothesis can be found that is consistent with the *training* data, it does not imply that the function will work well on unseen data. The ability of a hypothesis to give estimations on data points outside the training set is known as its generalization, and it is this property that is to be optimized.

The function, f, is often dependent on additional parameters, referred to as *model parameters*, that control the shape of the function. They are determined by a *cross validation* over the training set as is elucidated in the following section.

Cross Validation It is not necessarily desirable to achieve too high training accuracy, as that could lead to an over-fitted model which generalizes poorly. In order to improve the overall performance of the model, its parameters must be determined differently. A common way is to split the training data into n subsets of approximately equal size, train on $n-1$ subsets and validate on the remaining one. Training takes place n times where each of the subsets is used as a validation set. n validation accuracies are generated this way and their average is the estimated generalization error for the model parameters. These set of parameters that yield the lowest generalization error should be chosen when the final model is trained. This method[23] prevents over-fitting of the model but, alternatively, introduces additional computational time.

Data Entities When the data has to be filtered, as is the case in this study, care must be taken when splitting the data into training and test sets.

The data is split into approximately one hour chunks, each of which is to be used as an entity. The entity is filtered as a whole and used in either the training data or the test data.

Entities are subsequently randomly selected into training and test data sets at ratio 80% vs. 20% respectively.

5.2 Support Vector Regression

Support Vector Regression (SVR)[24, 25, 26, 27] is a learning machine that has yielded promising results in recent years. The attractiveness of SVRs stem from the process itself; first, the data is implicitly mapped, through the introduction of kernels of data point pairs, into a high dimensional feature space. In this space, a conventional linear regression can be applied to the mapped data, effectively handling noise and outliers implicitly. It is easy to find the linear function since the kernel ensures that the optimization problem will be convex. The corresponding function in the original data space

will be nonlinear, but its shape will depend on the choice of kernels. This can be performed with moderate computational efforts. The resulting model is sparse, i.e. comprised of only a few vectors, leading to a computationally efficient solution.

Problem Statement. In essence the ϵ-Support Vector Regression problem can be stated as the following optimization problem.

Define the linear ϵ-insensitive loss function by

$$L^{\epsilon}(y, f(\mathbf{x}, \mathbf{w})) = \max(0, |y - f(\mathbf{x}, \mathbf{w})| - \epsilon)$$

where $\mathbf{x}$ is a vector of input values, $\mathbf{w} \in \mathbb{R}^k$ is a vector of function parameters, ϵ is a real positive error tolerance value and

$$f : \mathbf{X} \times \mathbb{R}^k \to \mathbb{R}; \mathbf{x} \mapsto \langle \mathbf{w} \cdot \phi(\mathbf{x}) \rangle + b$$

where ϕ is a feature map (see below). It measures the quality of estimates by emphasizing on errors that are outside the distances of the true value.

Given $\{(\mathbf{x}_1, y_1), \ldots, (\mathbf{x}_n, y_n)\}$, a set of input/output data point pairs, the parameters $\mathbf{w}$ are chosen such that

$$\frac{1}{2}||\mathbf{w}||^2 + C \sum_{i=1}^{n} L^{\epsilon}(y, f(\mathbf{x}, \mathbf{w})) \tag{5.1}$$

is minimized for some values C and ϵ. An equivalent optimization problem form is as follows:

$$\begin{aligned} \min_{\mathbf{w},b,\xi,\xi^*} \quad & \frac{1}{2}||\mathbf{w}||^2 + C \sum_{i=1}^{n} (\xi_i + \xi_i^*) \\ \text{subject to} \quad & f(\mathbf{x}_i; \mathbf{w}) - y_i \leq \epsilon + \xi_i, \\ & y_i - f(\mathbf{x}_i; \mathbf{w}) \leq \epsilon + \xi_i^*, \\ & \xi_i, \xi_i^* \geq 0, i = 1, \ldots, n. \end{aligned}$$

where ξ_i and ξ_i^* are *slack variables* that measure the difference from the data points to the ϵ-insensitive tube (see figure 5.2)

The corresponding dual optimization problem can be expressed as follows:

$$\begin{aligned} \min_{\alpha,\alpha^*} \quad & \frac{1}{2}(\alpha - \alpha^*)^T Q(\alpha - \alpha^*) + \epsilon \sum_{i=1}^{n} (\alpha_i + \alpha_i^*) + \sum_{i=1}^{n} y_i(\alpha_i - \alpha_i^*) \\ \text{subject to} \quad & \sum_{i=1}^{n} (\alpha_i - \alpha_i^*) = 0, \\ & 0 \leq \alpha_i, \alpha_i^* \leq C, i = 1, \ldots, n. \end{aligned}$$

where Q is an $n \times n$ positive semidefinite matrix defined by the *kernel*:

$$Q_{ij} = K(\mathbf{x}_i, \mathbf{x}_j) := \langle \phi(\mathbf{x}_i) \cdot \phi(\mathbf{x}_j) \rangle \tag{5.2}$$

This is a convex optimization problem without any local minima with an efficient solution algorithm based on the Lagrangian theory.

The resulting function can be expressed as follows

$$\hat{f}(\mathbf{x}) = \sum_{i=1}^{n_{\text{sv}}} (-\alpha_i + \alpha_i^*) K(\mathbf{x}_i, \mathbf{x}) + b \tag{5.3}$$

where $-\alpha_i + \alpha_i^* \neq 0$ only for the vectors $\mathbf{x}_i$ located on the boundary of the ϵ-insensitive tube (see figure 5.2); namely the support vectors.

The feature map ϕ and the kernel K are explained further in the next paragraph.

Kernels. The feature map, ϕ, maps the input data into a high dimensional feature space F where there is a linear relationship between the data points (see figure 5.1):

$$X \ni \mathbf{x} = (x_1, \ldots, x_k) \mapsto \phi(\mathbf{x}) = (\phi_1(\mathbf{x}), \ldots, \phi_N(\mathbf{x})) \in F$$

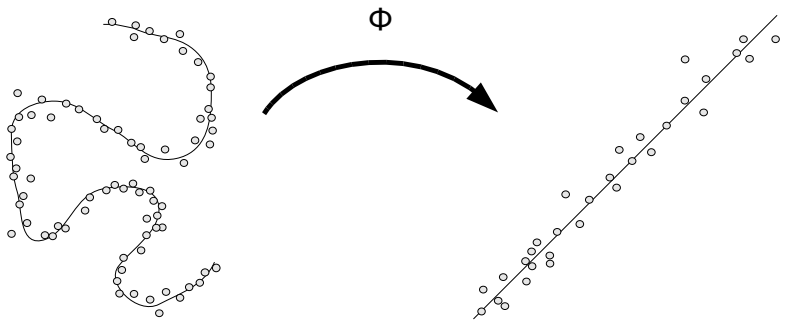

Figure 5.1: Data can be mapped into a higher dimensional feature space.

Determining ϕ can be a daunting task but from equation 5.2 it can be seen that there is no need to do that explicitly. By replacing the inner product with a kernel function defined on the original data space

$$K : X \times X \to \mathbb{R}; (\mathbf{x}_1, \mathbf{x}_2) \mapsto y$$

the data can be implicitly projected into a high dimensional feature space since this is the only place where the mapping enters into the dual optimization problem.

Kernels can be defined in various ways, as long as they satisfy the following conditions in order that they correspond to an inner product in the feature space. The kernel function must be *symmetric*:

$$K(\mathbf{x}_1, \mathbf{x}_2) = K(\mathbf{x}_2, \mathbf{x}_1)$$

and satisfy the following *inequality*

$$K(\mathbf{x}_1, \mathbf{x}_2)^2 \leq K(\mathbf{x}_1, \mathbf{x}_1) \cdot K(\mathbf{x}_2, \mathbf{x}_2)$$

for all $\mathbf{x}_i, \mathbf{x}_j \in X$. And, finally, the kernel matrix

$$\mathbf{K} = (K(\mathbf{x}_i, \mathbf{x}_j))_{i,j=1}^{n}$$

must be positive semi-definite.

The kernel effectively measures the similarity between data points. The most common kernels are the linear, polynomial, sigmoid and the Gaussian kernel (radial basis function (RBF)). The RBF kernel that will be used in this thesis measures the similarity between data points $\mathbf{x}_1$ and $\mathbf{x}_2$ as

$$K(\mathbf{x}_1, \mathbf{x}_2) = \exp(-\gamma||\mathbf{x}_1 - \mathbf{x}_2||^2) = \sum_{i=0}^{\infty} \frac{(-\gamma||\mathbf{x}_1 - \mathbf{x}_2||^2)^i}{i!} \tag{5.4}$$

where $\gamma > 0$ is a kernel parameter. Thus, equation 5.4 implies that the induced feature space is infinite dimensional.

SVR Generalization The aim is to optimize the generalization bounds given in equation 5.1. Figure 5.2 illustrates the ϵ-insensitive tube around the estimated function. Parameter ϵ determines the width of the ϵ-insensitive margin, used to fit the training data. It affects the number of support vectors where larger ϵ values imply fewer support vectors. C is a penalty parameter which determines the degree to which errors larger than ϵ are tolerated when finding the optimization solution. This parameter affects outliers and noisy data. The generalization error will depend both on C and the number of support vectors.

SVR Model. The solution model, i.e. the output from the learning algorithm, is comprised of support vectors that lie on the ϵ-insensitive tube (see figure 5.2). Model parameters C and ϵ depend on the data domain and are usually considered as an input from the user.

The kernel chosen for this study is the RBF kernel from equation 5.4. Apart from the model parameters C and ϵ, the kernel parameter, γ, has to be specified.

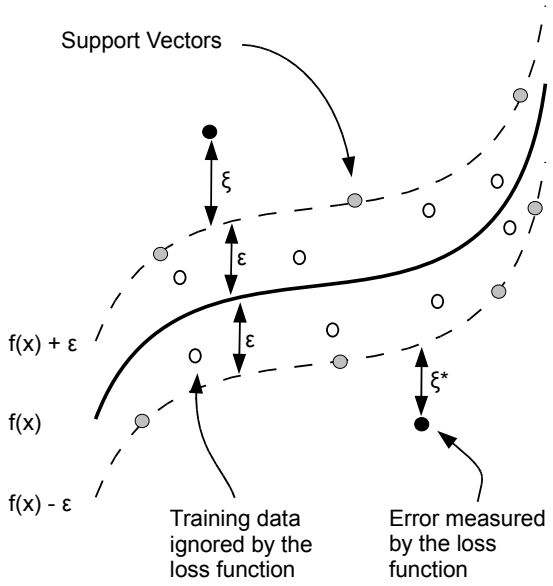

Figure 5.2: The ϵ-insensitive tube around the estimated function. The support vectors are located on the boundary of the tube.

5.3 k Nearest Neighbor

The k Nearest Neighbor (kNN) regression [28, 29, 30] consists of estimating the mean of the given output values at the k closest data points to a given point. The distance is a Euclidean distance metric where input parameter values are first normalized and subsequently given different weights to reduce the error and thus overcome the problem of the curse of dimensionality[28, 30].

Target Function. kNN is based on instance based approaches where the output from data point $\mathbf{x}$ will be estimated from the k nearest input points that are in the neighborhood. More precisely, the estimate of the output value for a input point $\mathbf{x}$ is the mean of the output values of the k nearest input points

$$\hat{f} : \mathbb{R}^n \to \mathbb{R}; \mathbf{x} \mapsto \frac{\sum_{i \in N_k(\mathbf{x})} f(\mathbf{x}_i)}{k}$$

where $N_k(x)$ denotes the set of the k input vectors that are closest to $\mathbf{x}$ in the training set.

Hence, kNN is an instance based model as the whole training set is stored and, generalization of the target function (i.e. the model) is not performed until the query instance is given. Therefore, the model is locally constrained and estimates differently for each query data point.

The advantage of this method is that no information is lost but, on the other hand, the cost of estimating new instances can be high if the training set is large.

Distance Metrics. The distance metric used to measure the k nearest input points to a given instance $\mathbf{x}$ is usually based on Euclidean distance metric:

$$d(\mathbf{x}_1, \mathbf{x}_2) = \sqrt{\sum_{i=1}^{k} (x_{1i} - x_{2i})^2} \tag{5.5}$$

where $\mathbf{x}_1$ and $\mathbf{x}_2$ are input points from the training set.

Figure 5.3 illustrates how the k nearest input points are determined with the Euclidean distance metric.

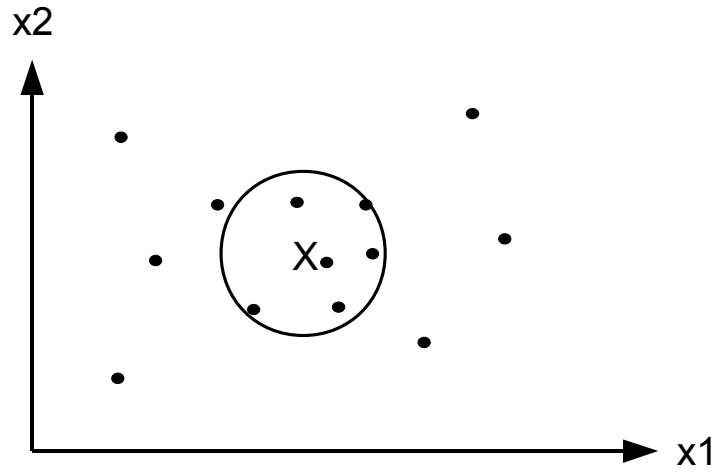

Figure 5.3: k nearest input points to the instance $\mathbf{x}$ determined with a Euclidean distance metric.

Often, the k nearest input points are given weights, according to their distance to the query instance $\mathbf{x}$, by assigning higher weights to closer neighbor input points. The distance-weight method is commonly defined as follows:

$$\hat{f}(\mathbf{x}) = \frac{\sum_{i=1}^{k} w_i f(\mathbf{x}_i)}{\sum_{i=1}^{k} w_i} \tag{5.6}$$

where

$$w_i = \frac{1}{d(\mathbf{x}, \mathbf{x}_i)^2}$$

If $\mathbf{x} = \mathbf{x}_i$ the output estimation can be assigned the training output value, $\hat{f}(\mathbf{x}) = f(\mathbf{x}_i)$.

Coordinate Weights. One disadvantage with the kNN method is how poorly it scales with an increased number of coordinates. The distance of the nearest data points are based on all input parameters even though some of the input parameters are irrelevant. Data points that are in essence identical with respect to important input parameters could be distant from one another in higher dimensional space. The distance between points will be dominated by irrelevant input parameters resulting in an unreliable distance metric. This problem is known as the *curse of dimensionality*.

An approach to remedy this problem is to normalize the whole data set to a certain interval, e.g. $[-1, 1]$. Another is to weight the coordinates of the input parameters:

$$d(\mathbf{x}_1, \mathbf{x}_2) = \sqrt{\sum_{i=1}^{k} w_i (x_{1i} - x_{2i})^2} \tag{5.7}$$

This method stretches the i-th axis with a weight w_i. Input parameters that should be more influential receive a higher weight while the less relevant ones receive lower weights. Figure 5.4 illustrates how the distance to nearest data points changes when one axis is lengthened.

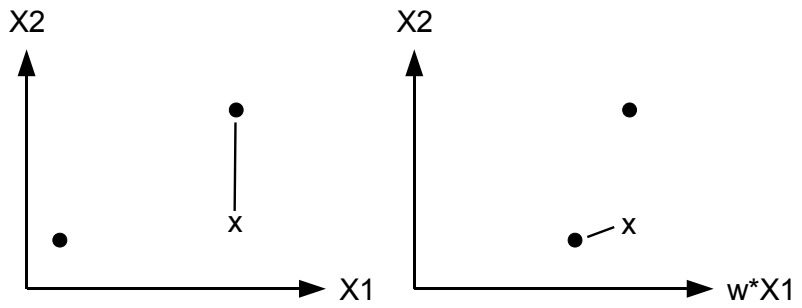

Figure 5.4: The results from the distance metric can change if the weights are applied to the coordinates.

kNN Model. The choice of k is a compromise between wanting to obtain a reliable estimate and wanting the k nearest data points to be as near the query instance, $\mathbf{x}$, as possible to ensure similarity. Thus, the model-parameters are k and the weights for the normalized coordinates from equation 5.7. The distance metrics from equations 5.5 and 5.6 are both used in this thesis.

5.4 Other Black-box Models

The main attention, in this study, has thus far been on the SVR and the kNN models. This section describes other black-box models that have also been applied. These are *Classification and Regression Trees* (CART), *Bagging* and *Artificial Neural Networks* (ANN).

Decision Trees. Classification and Regression Trees[28, 30, 31] are founded on hierarchical concepts where the most important input parameter is determined at each node and a choice is made on how to proceed dependent upon the value of this parameter. The tree is comprised of *inner nodes* where the choice is made and *leaf nodes* where the output value is specified. Figure 5.5 illustrates a simple regression tree.

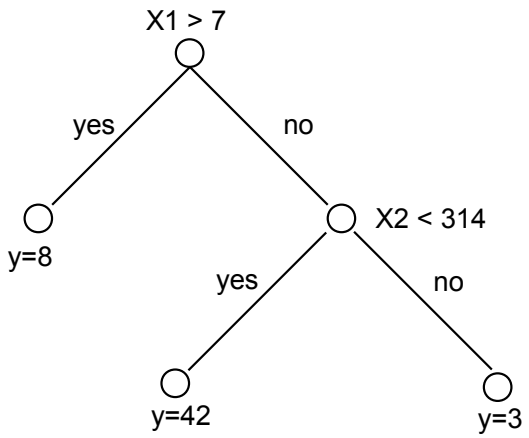

Figure 5.5: A very simple regression tree. The choice is made on how to proceed down the tree dependent upon the value for the most important parameter at each node. The output value is specified in the leaf nodes.

The only model parameter used in this study is a number n such that nodes must have n or more observations to be split into two descendant nodes[1].

Bagging. The CART model is unstable in the sense that a slight difference of an input value could render a completely different tree. A modification to the CART model is to generate a *bag*[32, 33] of diverse models which is less unstable. This is accomplished by rendering a model from samples that have been randomly sampled from the training set with replacement. The mean from the output of the models determine the output of the total model for a given data point.

[1] See `treefit` in Matlab

The model parameters are the number of bags and the number n as readily described above in the CART section.

Artificial Neural Network. Artificial Neural Network[30] (ANN) is a feed-forward back-propagation network of nodes which is capable of expressing various non-linear functions.

In a network with one hidden layer with m nodes the function to be learned takes the form

$$y = \sum_{i=1}^{m} \tilde{w}_i \tanh(\sum_{j=1}^{n} w_{ij} x_j + w_{i0}) + \tilde{w}_0$$

Figure 5.6 illustrates the network that is used in this thesis.

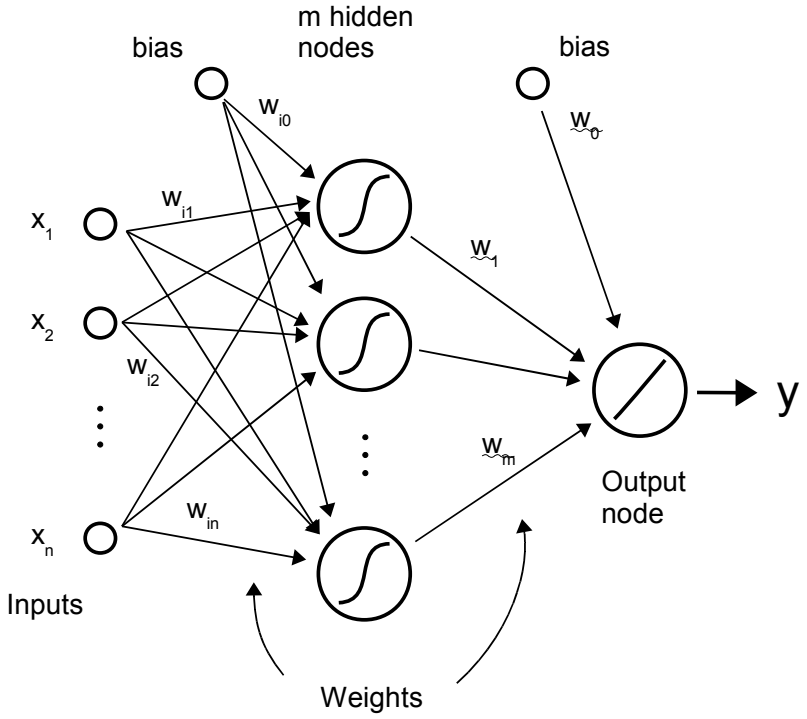

Figure 5.6: A network of nodes with n input parameters, m hidden nodes and one output node.

The weight and bias values, i.e. the function parameters, are determined by the Levenberg-Marquardt back-propagation algorithm[2]. It updates the weights at each iteration step, decreasing the training error

[2]See `trainlm` in Matlab

in the process. This can lead to an over-fitted model since the function can be approximated to an arbitrarily degree of accuracy, by choosing m large enough.

Therefore, the model parameters are the number of nodes in the hidden layer and the number of iterations performed by the training algorithm.

5.5 Implementation

The SVR model implementation is based on *libSVM* [27]. The implementation for the other machines is embedded in Matlab[3].

The model parameters are determined with a simple grid search over possible parameter values and a 5-fold cross validation on the training data to choose the parameters that give the best fit.

5.6 Summary

This chapter briefly describes the learning machines employed in this thesis. The support vector regression is a model that, through kernels, maps data with non-linear relationship into a feature space where the data has a somewhat more linear relation. In this space, a conventional linear regression can be applied to the mapped data ensuing in a function in the original data space that is nonlinear. The k Nearest Neighbor model consists of estimating the mean of the given output values at the k closest data points to a given point. Other machines are also introduced for comparison to the SVR and the kNN models.

The black-box models that have been introduced in this chapter will be used to simulate the shaft power in the next chapter.

[3]See `http://www.mathworks.com`.

Chapter 6

Experimental Study

In this chapter, the black-box models presented in Chapter 5 are used to simulate how the shaft power of the vessel depends on various external and operational conditions, using the data set described in Chapter 3 after it has been preprocessed according to the description in Chapter 4. The aim is to be able to derive an optimal pitch configuration with respect to fuel usage for given values of all the remaining external and operational parameters. The chapter commences with a discussion on input parameter selection, followed by results from the model parameter search. Subsequently, modifications to the SVR and kNN models are introduced and tested. Predictive results for the optimal pitch are then presented and the chapter concludes by proposing the introduction of a prediction score function.

6.1 Parameter Selection

The model selection must be based on as few features as possible without sacrificing too much information on the process. Even though a feature contributes to a model it might be discarded since the contribution is marginal, while adding it will add to the complexity of the model. Numerous feature selection methods were applied in an attempt to reduce the number of input parameters.

Weka The WEKA project[34] contains a feature selection method where a combination of sequential forward selection and sequential backward selection is applied to select a subset of parameters that are most discriminative. It searches the space of parameter subsets by greedy hill-climbing augmented with a backtracking facility.

AIC The Akaike Information Criterion[35] can be used in conjunction with a simple linear least-squares model on all permutations of input parameters. AIC is defined as

$$\mathrm{AIC} = n \log(\mathrm{SS(E)}/n) + 2d$$

where d is the number of input parameters, n is the number of data points and SS(E) is the sum of squared errors

$$\mathrm{SS(E)} = \sum_{i=1}^{n} (y_i - \hat{y}_i)^2$$

A combination of features with the lowest AIC value is considered to contribute the most to the model without sacrificing too much information.

CART The CART model constructed from the training data can be used to determine whether an input parameter should be included or not by inspecting whether it is used to construct the decision tree (see `treefit` in Matlab).

Each of these methods returned a different preference of input parameter selection. Consequently, it was decided to use all the available input parameters. Figure 6.1 illustrates how the setup is for all black-box models.

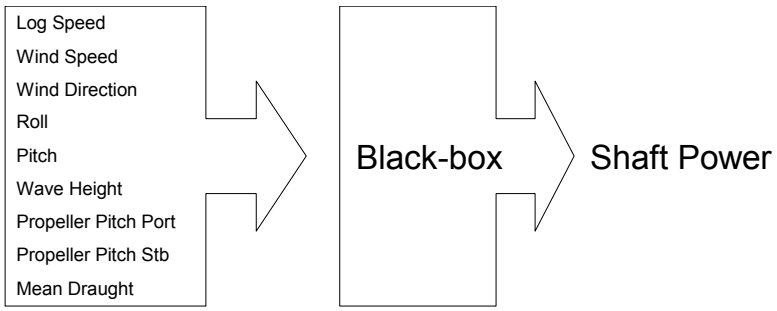

Figure 6.1: The setup for all black box models.

6.2 Model Parameters

The results from a grid search of the optimal model parameters are presented in this section. Model parameters for the SVR and kNN models are given special attention as they will be used in section 6.3 to construct a new coordinate-weighted distance metric.

6.2.1 SVR Parameters

The model parameters for the SVR model turn out to be

$$(\gamma, \epsilon, C) = (0.3, 100, 7000) \tag{6.1}$$

6.2.2 kNN Parameters

The model parameters for the kNN model are

$$k = 20, \quad \mathbf{w} = (0.1, 0.1, 0.01, 0.1, 1, 0.1, 5, 5, 0.1)$$

Due to time constraints, a thorough search for the coordinate weights with the intention of finding the best fit for the kNN model were not performed. Only values from the set $w_i \in \{0.01, 0.1, 1, 5\}$ were tested which limits the hypothesis space considerably.

The parameters corresponding to the coordinate weights are shown in table 6.1. The propeller pitch parameters turn out to be assigned a dominant

Input Parameter	Weight
Log Speed	0.1
Wind Speed	0.1
Wind Direction	0.01
Roll	0.1
Pitch	1
Wave Height	0.1
Propeller Pitch Port	5
Propeller Pitch Stb.	5
Mean Draught	0.1

Table 6.1: The parameters corresponding to the coordinate weights in the kNN model.

weight value, indicating that they are the most important input parameters in detecting optimal pitch values. Significantly, in terms of this study, the pitch parameter is likewise quite important as it has a higher value than the remaining parameters.

6.2.3 Parameters of other Models

In the *bagging* method, the number of bags turns out to be 20. In ANN, the number of hidden nodes turns out to be 20. These numbers are not particularly intuitive and, therefore, will not be discussed further.

6.3 Augmented Distance Metric

Instinctively, use can be made of the parameters obtained for the SVR model in the kNN model and vice versa

- add the coordinate weights from the kNN model to the distance metric in the RBF kernel for the SVR model, and

- introduce a RBF induced distance-weight to the k nearest points in the kNN model.

This reflects, to a certain degree, the similarities between these two model types. A key ingredient of both methods is how one estimates the importance of neighboring points from the appropriate measure of distance to them.

These modifications are described in detail in the following subsections.

6.3.1 Coordinate Weighted RBF Distance in SVR

A new kernel based on the coordinate weights, $\mathbf{w} = (w_1, ..., w_9)$, from the kNN model can be constructed for the SVR model:

$$K(\mathbf{x}_i, \mathbf{x}_j) = e^{-\gamma||\mathbf{W}\cdot(\mathbf{x}_i - \mathbf{x}_j)^{\mathrm{T}}||^2}$$

where $\mathbf{x}_i$ and $\mathbf{x}_j$ are data points, γ is from equation 6.1 and

$$W = \begin{pmatrix} w_1 & \cdots & 0 \\ \vdots & \ddots & \vdots \\ 0 & \cdots & w_9 \end{pmatrix} \tag{6.2}$$

The difference between this kernel and the RBF kernel is the introduction of coordinate weights that are applied to the input parameters.

6.3.2 RBF Induced Weight Distance in kNN

A RBF induced weight distance metric for the k nearest neighborhood points is defined as follows

$$\omega_j = \frac{e^{-\gamma||\mathbf{W}\cdot(\mathbf{x} - \mathbf{x}_j)^{\mathrm{T}}||^2}}{\sum_{i=1}^{k} e^{-\gamma||\mathbf{W}\cdot(\mathbf{x} - \mathbf{x}_i)^{\mathrm{T}}||^2}}, \quad j = 1, \ldots, k$$

where $\mathbf{W}$ is from equation 6.2 and γ is the same as used in the SVR model (equation 6.1). This method adds weights to the nearest points in a similar fashion as to the SVR model.

The results from these modifications are presented with other model results in section 6.5.

6.4 Model Quality

The root mean square (RMS) error is the model quality metric of choice:

$$\mathsf{RMS}(e) = \sqrt{\frac{\sum_{i=1}^{n} e_i^2}{n}}$$

where the error $e_i = (y_i - \hat{y}_i)$ for point i, $i = 1, ..., n$, is the difference between the observed response value y_i and the estimated response value $\hat{y}_i$.

6.5 Results

The results from this study are twofold. First, the results of the overall quality of the model for shaft power prediction are displayed. Subsequently, the results on how the models perform in predicting the optimal pitch configuration are presented.

6.5.1 Predictive Results

Table 6.2 shows how all models perform on unseen test data and how large their error RMS is compared to the RMS of the power shaft values. All

Model	Error RMS	% of total RMS
ϵ-SVR	289	2.00
Weighted Coordinates ϵ-SVR	282	1.95
Normal kNN	373	2.58
Weighted Coordinates kNN	277	1.91
Euclidean Distance-Weight kNN	372	2.58
RBF-Distance-Weight kNN	278	1.92
CART	369	2.55
Bagging	291	2.01
ANN	315	2.18
Shaft Power	14442	

Table 6.2: RMS error results from black-box models.

models perform adequately, indicating that they are viable as a model that can be used to predict the shaft power usage for different configurations of the pitch. Figure 6.2 depicts the prediction result for the weighted coordinates kNN model (the figure for other models is quite similar). The black line is the predicted shaft power, which essentially overlaps the original shaft power measurements, displayed as a thick grey line. The error is shown below.

Figure 6.3 illustrates an alternative view of the error for the weighted coordinates kNN model. The histogram of the shaft power estimation error is on the figure to the left side. On the right side, the estimated shaft power is plotted against the observed shaft power. It is interesting to see that there seems to be a pattern in the error for some cases. This may indicate that additional input parameters are needed for the black-box models that could explain this error pattern.

It is of interest to note, that the introduction of weights for different normalized input parameter values reduces the RMS error significantly, in the cases of the kNN model and the SVR model. No attempts were, however, made to find the SVR parameters that give the weighted coordinates SVR model the best fit, leaving it open for improvements. It is also of interest to

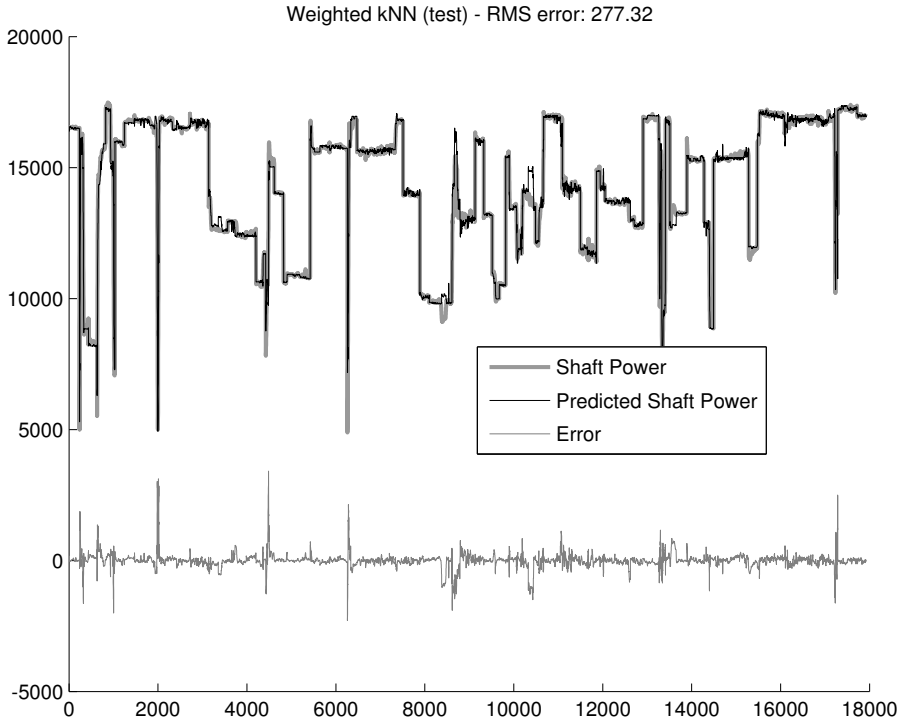

Figure 6.2: Shaft power prediction using the weighted coordinates kNN model. The black line is the predicted shaft power, which essentially overlaps the original shaft power measurements, displayed as a thick grey line. The error is shown below.

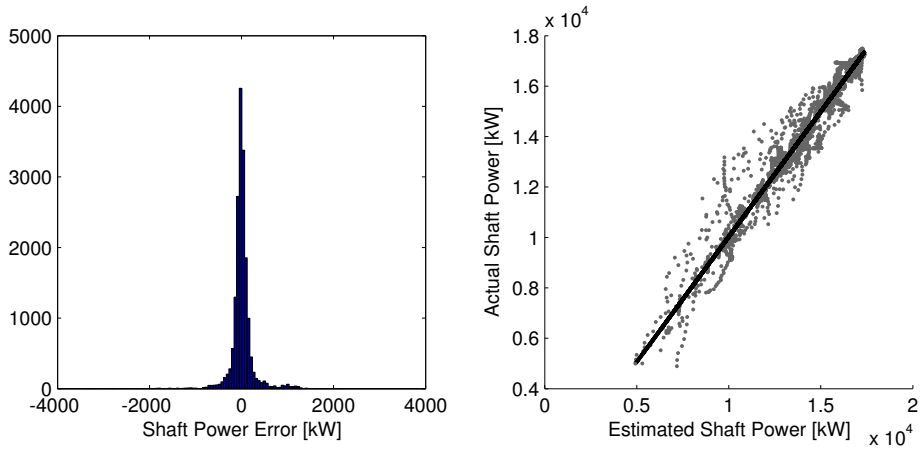

Figure 6.3: The histogram of the shaft power estimation error is on the figure to the left and, a scatter plot of the estimated shaft power plotted against the observed shaft power to the right.

note that using a distance weight on the neighboring points does not change the performance of the kNN model at all.

6.5.2 Optimal Pitch Configuration

Although the model thus predicts shaft power satisfactorily for unseen data of input parameters, it does not necessarily imply that it will accurately predict variations on shaft power when changing the pitch while keeping other input variables fixed. Figure 6.4 depicts how this prediction can be in certain situations.

The point `X` marked in the figure corresponds to a data point where all the input parameters, as well as the shaft power, are known. The vertical segment through the point shows the overall RMS error of 290. The curves then show how the predicted shaft power varies according to all models when all the input parameters except for the pitch are held constant at these values. The models are not predicting convincingly for pitch values far from

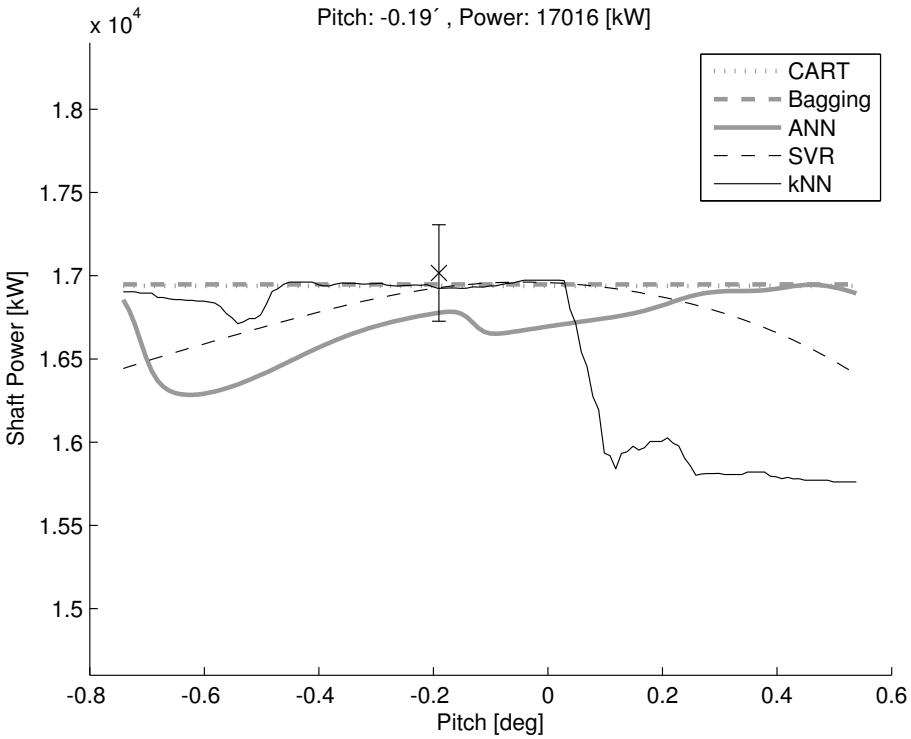

Figure 6.4: An example of a poor shaft power prediction for pitch values far from zero. The vertical segment through the known data point, marked with `X`, shows the RMS error of 290.

zero. They all suggest that extreme pitch values, possibly beyond physical

capacity, are the optimal ones. The problem stems from the external or operational conditions that the point presents. There are not enough points in the data set that include similar conditions but with different pitch values. This causes the model to give predictive results induced from data points where the values of the remaining input variables differ significantly from the fixed ones. The data range is not broad enough to generate black-box models that can predict the dependence of shaft power on pitch for these conditions.

Alternatively, figure 6.5 illustrates where there is a general consensus between the SVR, the kNN and the ANN models on a realistic location of the optimal pitch, while the CART and the bagging models do not yield useful information in determining the optimal pitch. This could be useful if

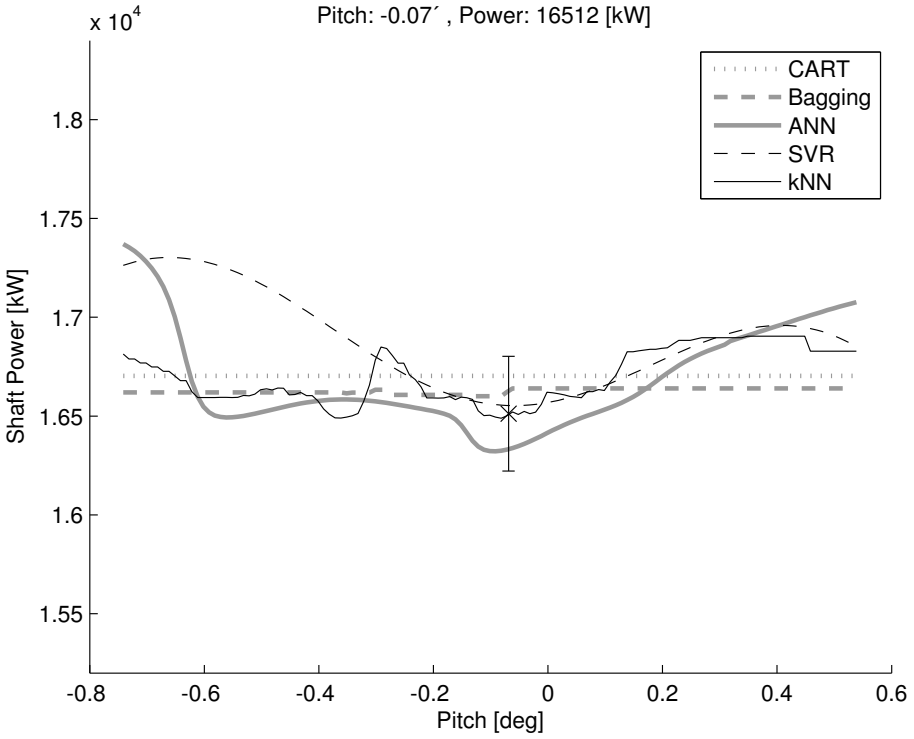

Figure 6.5: An example of the SVR, kNN and ANN models agreeing on the optimal pitch location while the CART and the bagging models are not useful.

the vessel happened to be incorrectly trimmed.

Selected Model Types

The SVR and kNN model types will be used from now on as the other model types are performing similarly or worse. For clarity, figures 6.4 and 6.5 are

displayed again in figure 6.6 where only the results from the kNN model and the SVR model are illustrated:

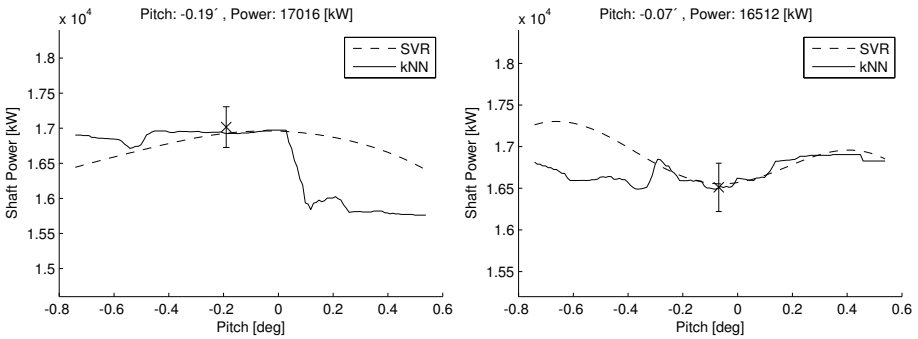

Figure 6.6: Shaft power estimation for various pitch configurations illustrated for the kNN model and the SVR model.

kNN Prediction Score

The variation of the prediction curves indicates a need of introducing some form of a prediction score, for a generated data point, reflecting the closeness of neighboring data points. It can be chosen such that values become 1 when the neighboring points coincide with the generated point. Equation 6.3 proposes a prediction score function of this kind, based on the RBF-distance-weighted kNN model, for a pitch value p:

$$S(p) = \frac{1}{k}\sum_{i=1}^{k} e^{-||\mathbf{W}\cdot(\mathbf{x}_i - \tilde{\mathbf{x}}(p))^{\mathrm{T}}||^2} \in]0,1] \tag{6.3}$$

The score is the average of the scaled weighted distance from a given point, $\tilde{\mathbf{x}}(p)$ with pitch p, to k nearest points, $\mathbf{x}_i$, $i = 1, ..., k$. The weights in the matrix, $\mathbf{W}$, are the same as in equation 6.2. The data points $\tilde{\mathbf{x}}(p)$ are generated input points where all the input parameters, excluding the pitch, are held constant.

Figure 6.7 illustrates this score function, displayed along with the model predictions. The score function suggests that the kNN model predicts adequately for pitch values from -0.4 to -0.05. If the vessel happened to be trimmed around -0.4 this figure would indicate that the ship should instead be trimmed around -0.1, in order to reduce the shaft power consumption by approximately 800 kW, which is outside the error margin of 300 kW. A power reduction of 500 kW for 20 hours (one trip) implies a 1.9 MT savings in fuel usage, given that the engines are running at 190 g/kWh in specific fuel consumption; a reduction of 3.4% or \$540 if the price for 1 MT is \$300[1].

[1]See `http://www.bunkerworld.com`

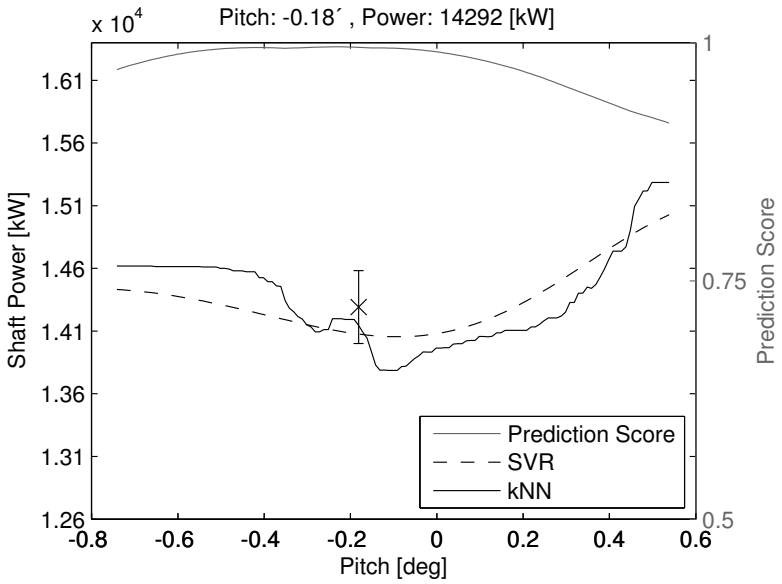

Figure 6.7: An example of how a prediction score can be displayed along with predicted values. The score indicates reliable predictions of values from -0.4 to -0.05.

In particular, the score function must indicate when the shaft power estimations should be discarded.

Figure 6.8 illustrates when the score function is too far from 1, indicating that the shaft power estimations are unreliable. The figure suggests that a cut-off value as high as 0.99 may be needed to indicate reliable predictions but, this remains to be investigated more fully.

Sensitivity of the Models

As a further indication of the potential usefulness of these types of models a sensitivity analysis has been carried out assessing how much the optimal pitch values, dependent upon the models, change when one of the input parameter values are altered while keeping the remainder fixed. The base case for this analysis is given in table 6.3. These values, denoted by μ_i, are the average values of each input parameter value in the training data set. Also shown is the standard deviation, σ_i, for all input parameters except the Log Speed and the Propeller Pitches. The σ_i for the Log Speed and the Propeller Pitches were determined empirically, since changing one of these parameters by the proposed standard deviation is in effect unrealistic without changing the other two as well.

The SVR-model and the kNN-model almost agree on the optimal pitch value for this base case, being -0.07 according to the SVR model and -0.09

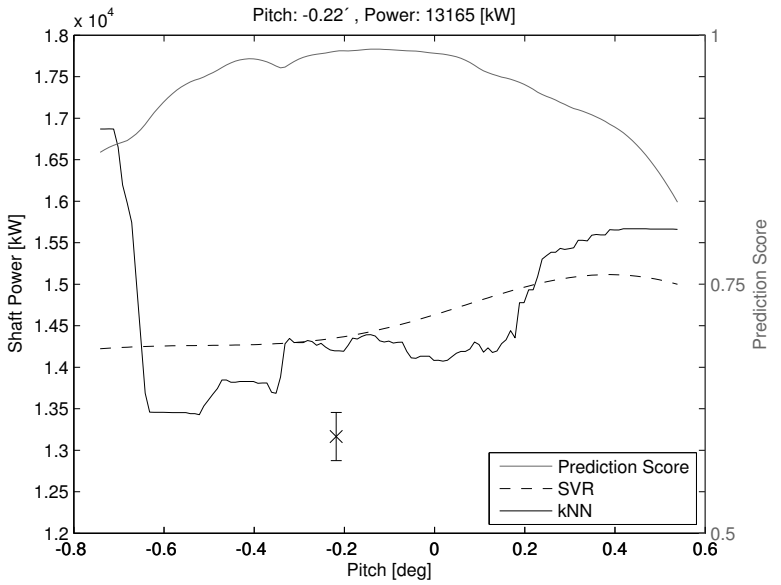

Figure 6.8: An example of how a prediction score can be used to indicate that the shaft power estimations are unreliable.

	μ_i	σ_i
Log Speed	17.2	1.6
Wind Speed	11.2	6.4
Wind Direction	213	30
Roll	-0.73	0.9
Wave	1.34	1.3
Propeller Pitch Prt	80	2
Propeller Pitch Stb	78	2
Mean Draught	6.51	0.1

Table 6.3: The average of the input parameters in the training data set is given in the μ_i column. The σ_i column lists the standard deviation for all input parameters except the Log Speed and the Propeller Pitches which, in turn, were determined empirically.

according to the kNN model.

We now calculate for each model the optimal pitch value by replacing in turn each input parameter value by $\mu_i - \sigma_i$ and $\mu_i + \sigma_i$. These results are shown in table 6.4, which also shows the offset in the optimal pitch value from the baseline value in each case.

	SVR				kNN			
	$-\sigma_i$	Δ	$+\sigma_i$	Δ	$-\sigma_i$	Δ	$+\sigma_i$	Δ
Log Speed	0.06	0.13	-0.15	-0.08	-0.01	0.08	-0.08	0.01
Wind Speed	-0.08	-0.01	-0.05	0.02	-0.23	-0.14	-0.12	-0.03
Wind Dir.	-0.09	-0.02	-0.04	0.03	-0.06	0.03	-0.09	0
Roll	-0.02	0.05	-0.12	-0.05	-0.08	0.01	-0.08	0.01
Wave	-0.01	0.06	-0.10	-0.03	-0.05	0.04	-0.32	-0.23
Pr.Pitch Prt	-0.10	-0.03	-0.03	0.04	0.05	0.14	-0.18	-0.09
Pr.Pitch Stb	-0.07	0	-0.07	0	-0.12	-0.03	-0.04	0.05
Mean Draught	-0.10	-0.03	-0.04	0.03	-0.10	-0.01	-0.04	0.05

Table 6.4: The $\pm\sigma_i$ columns list the optimal pitch values for each model, where the input parameter value, i, has been replaced by $\mu_i \pm \sigma_i$, and Δ designates the offset of the optimal pitch configuration from the optimal pitch configuration for the base case.

This table brings out a number of noteworthy facts:

- The results of the SVR-model are smoother, and possibly more robust, in that the optimal baseline value lies in all cases between the optimal values of the two extreme cases. For the kNN model this does not hold true in the cases of Log Speed, Wind Speed and Roll. This is also reflected by typical model curves as those shown in figure 6.7.
- There a considerable discrepancy in the optimal values between the two models, in particular in the cases of Wind Speed, Wave and Propeller Pitch Port.
- The highest offset value for the smoother SVR-model is only 0.06, apart from the case of Log Speed.

6.6 Summary

The black-box models perform well on unseen test data, indicating that they are viable in predicting the shaft power for various pitch values. However, in some cases, they do not perform adequately in finding the optimal pitch configuration. Nevertheless, even though the models cannot predict fuel consumption accurately for all occasions, there is evidence that they can aid the captain when the trim of the vessel is incorrectly configured. Specifically, if a prediction score would be used to indicate whether the estimate of the optimal pitch configuration is reliable.

Chapter 7

Conclusion

This thesis examined the feasibility of using black-box models to simulate the power consumption of a vessel for different trim values in an attempt to derive an optimal trim configuration with respect to fuel usage. The objective was to create a simulation model to be used in a decision support system for potential fuel usage savings.

The investigation was based on empirical data sampled at the passenger and freight vessel, Norröna, which has a cruising schedule in the North-Atlantic Ocean. The data chosen for this study were those considered to contribute primarily to the total resistance of the vessel.

Careful attention was given to the preprocessing of the data. Data segments corresponding to the voyages of the vessel were isolated. Those that contained gaps were either patched or removed. Data series that contained incorrect measurements were corrected. Noisy data were filtered and outliers were removed. Finally, all the data series were synchronized in time to make them well formed for black-box models.

Five models types were tested but two of them were considered specifically; the support vector regression model and the k nearest neighbor model. The models' performance for estimating the shaft power for unseen data turned out to be adequate. Subsequently, they were used to estimate the variability of the power consumption with different trim configurations. They turned out to be unreliable when estimating the power consumption for trim values outside the range of the data set. An introduction to a prediction score was presented to indicate the proximity of the data that the models based their estimation on.

Conclusion

In this study, black-box models did not perform adequately in finding the optimal trim configuration in some cases. The main reason is the nature of the data set where the range of some of the parameters was too narrow to generate a complete model. Sampling more data to broaden the data set is

not necessarily achievable, since some of the parameters cannot be controlled due to external conditions.

Even though the models cannot predict fuel consumption accurately in all cases, there is evidence that it can aid the captain when the trim of the vessel is incorrectly configured, in particular, if the prediction score would be used to indicate whether the estimate of the optimal trim configuration is reliable.

A typical application would be if the vessel is cruising in calm weather and the trim is incorrectly configured. The decision system would then indicate to the captain that the vessel is indeed improperly trimmed and that he could enhance the energy efficiency by trimming the vessel correctly.

The method presented here can likewise be applied to other types of vessels such as cruise liners, cargo ships and tank ships but the models must be adapted for each ship. The aim is to make such models part of an overall energy management system on board marine vessels.

7.1 Future Work

The sensitivity of the models must be further assessed by observing how the optimal trim value changes with different input parameter values under the normal operating condition of the vessel. The coordinate weights should be tuned better, as well, as their search space was reduced considerably due to time constraints. A more elaborate method for determining them should be considered instead of the simple grid search.

An application of this method would introduce a problem, regarding the data behind the models, which must be solved. The physical attributes of a vessel are continually changing over the course of time. The resistance factors of the vessel are likewise continually changing. This would render the models useless if they were not retrained, as the data that rendered them will become obsolete. An autonomous method should be devised, in order to retrain the models at specific intervals to update the models.

Likewise, a graphical user interface must be designed to relay the decision support messages in a proper and concise manner. The relationship between the prediction score function and the model estimates must, in particular, be considered more closely.

Other types of vessels should be subjected to this method for comparison reasons. Cargo ships and oil tankers are interesting subjects as their trim configuration are variable compared to passenger vessels.

Applying these models in conjunction with white-box models should also be considered. They could aid the predictive capabilities of the black-box models for data points outside the proximity of the data set. Moreover, they could estimate the physical capacity of the hull, preventing the vessel from incorrect trim configurations.

Bibliography

[1] Meijers JHC. Journée JMJ. Ship routeing for optimum performance. Number 529-P. Transactions IME, Conference on Operation of Ships in Rough Weather, 1980.

[2] Hellström T. Optimal pitch, speed and fuel control at sea. *Journal of Marine Science and Technology*, 12(2):71–77, 2004.

[3] Hallgrímsdóttir H. Minimal cost ship routing. Master's thesis, University of Iceland, 2007.

[4] Rocchi R. Delivered power - trim and sinkage - ship hull forms: an analysis of the effects of the trim variations on the power performance of a class of modern container ships. In *Transactions on the Built Environment*, volume 5, 1994.

[5] Journée JMJ. Review of the 1985 full-scale calm water performance tests onboard m.v. mighty servant 3. Technical Report 1361, revision 07-11-2003, Ship Hydromechanics Laboratory, Delft University of Technology, August 2003.

[6] Verleg GJH. Journée JMJ, Rijke RJ. Marine performance surveillance with a personal computer. Technical Report 753-P, Ship Hydromechanics Laboratory, Delft University of Technology, Automation Days 87, Finish Society of Automatic Control, Helsinki, Finland, May 1987.

[7] Comstock JP., editor. *Principles of Naval Architecture*. Society of Naval Architects and Marine Engineers, New York, 1967.

[8] Varyani KS. Squat effects on high speed craft in restricted waterways. *Ocean Engineering*, 33(3-4):365–381, 2006.

[9] 6th Annual Green Ship Technology. *Energy and Environmental Efficiancy of Ship Operations*, Hamburg, Germany, March 2009.

[10] Tavakoli MT Seif MS. New technologies for reducing fuel consumption in marine vehicles. In *XVI symposium SORTA2004*. 2004.

[11] Thorsteinsson JA. *Modelling of Fishing Vessel Operation for Energy System Optimisation.* PhD thesis.

[12] Stefánsson G. Design and implementation of a equation solver for an energy management system. Master's thesis, University of Iceland, 2004.

[13] Mennen GGJ. Holtrop J. An approximate power prediction method. *International Shipbuilding Progress*, 29(335):166–170, 1982.

[14] Holtrop J. A statistical re-analysis of resistance and propulsion data. *International Shipbuilding Progress*, 31(363):272–276, 1984.

[15] Faltinsen OM. Steen S. Added resistance of a ship moving in small sea states.

[16] Isherwood RM. Wind resistance of merchant ships. *Trans. of the Royal Institution of Naval Architects*, 115:327–338, 1972.

[17] Kristjánsson LA. Modeling of powering requirements for a pelagic trawler. Master's thesis, University of Iceland, 2005.

[18] Sævarsdóttir H. Grey box modeling and operational fuel optimization of a container vessel. Master's thesis, 2007.

[19] Man and BW. *Basic principles of ship propulsion*, 2005.

[20] Arribas FP. Some methods to obtain the added resistance of a ship advancing in waves. *Ocean Engineering*, 34:946–955, 2006.

[21] The Schottel Group. http://www.schottel.de/uploads/PDF1234949735.pdf.

[22] Hutcheson MC. *Trimmed Resistant Weighted Scatterplot Smooth.* Cornell University, 1995.

[23] Cover TM. Learning in pattern recognition. In Satoshi Watanabe, editor, *Methodologies of Pattern Recognition*, pages 111–132, New York, 1969. Academic Press.

[24] Vapnik V. Boser BE, Guyon I. A training algorithm for optimal margin classifiers. In *COLT '92: Proceedings of the fifth annual workshop on Computational learning theory*, pages 144–152, Pittsburgh, Pennsylvania, United States., 1992. ACM.

[25] Shawe-Taylor J. Christianini N. *An Introduction to Support Vector Machines and other kernel-based learning methods.* Cambridge University Press, Cambridge, UK, 2000.

[26] Schölkopf B. Smola AJ. A tutorial on support vector regression. *Statistics and Computing*, 2008.

[27] Lin C. Chang C. Libsvm: a library for support vector machines. Technical report, Department of Computer Science and Information Engineering, National Taiwan University, June 2007.

[28] Stork D. Duda R, Hart P. *Pattern Classification, Second Edition*. John Wiley & Sons, Inc., USA, 2001.

[29] Fischer FP. Patrick EA. A generalized k-nearest neighbor rule. *Information and Control*, 16(2):128–152, 1970.

[30] Mitchell TM. *Machine Learning*. McGraw-Hill Higher Education, 1997.

[31] Olshen R Stone C. Breiman L, Friedman J. *Classification and Regression Trees*. Wadsworth, 1984.

[32] Bishop CM. *Pattern Recognition and Machine Learning*. Springer, 2006.

[33] Breiman L. Bagging predictors. *Machine Learning*, 26(2):123–140, 1996.

[34] Weka: Datamining software. http://www.cs.wakato.ac.nz/ml/weka.

[35] Smyth P. Hand D, Mannila H. *Principles of Data Mining*. MIT Press, 2001.